FIŞĂ DE AUTOEVALUARE

privind standardele minimale pe domenii ale Universităţii, pentru posturile de cercetare

ANEXA 2

FACULTATEA DE CHIMIE	
ASISTENT DE CERCETARE	2 articole ştiinţifice publicate în extenso în reviste internaţionale, din care 1 în reviste cotate *Web of Science* cu factor de impact

1. Amarandei, C., Negru, A. G., Soroaga, L. V., Cucu-Man, S. M., Olariu, R. I., Arsene, C., Assessment of Surface Water Quality in the Podu Iloaiei Dam Lake (North-Eastern Romania): Potential Implications for Aquaculture Activities in the Area, *Water*, 13(17), 2395, **2021**. DOI: 10.3390/w13172395 — Factor impact: **3.103**
2. Grira, A., Amarandei, C., Romanias, M.N., El Dib, G., Canosa, A., Arsene, C., Bejan, I.G., Olariu, R.I., Coddeville, P., Tomas, A., Kinetic measurements of Cl atom reactions with C_5–C_8 unsaturated alcohols, *Atmosphere*, 11, 256, **2020**. DOI:10.3390/atmos11030256 — Factor impact: **2.686**

Doctorand Cornelia AMARANDEI

water

MDPI

Article

Assessment of Surface Water Quality in the Podu Iloaiei Dam Lake (North-Eastern Romania): Potential Implications for Aquaculture Activities in the Area

Cornelia Amarandei [1,2], Alina-Giorgiana Negru [2], Laurentiu-Valentin Soroaga [1,2], Simona-Maria Cucu-Man [1], Romeo-Iulian Olariu [1,2] and Cecilia Arsene [1,2,*]

[1] Department of Chemistry, Faculty of Chemistry, "Alexandru Ioan Cuza" University of Iasi, 11 Carol I, 700506 Iasi, Romania; cornelia.amarandei@uaic.ro (C.A.); laurentiu.soroaga@uaic.ro (L.-V.S.); sman@uaic.ro (S.-M.C.-M.); oromeo@uaic.ro (R.-I.O.)

[2] Integrated Centre of Environmental Science Studies in the North Eastern Region, "Alexandru Ioan Cuza" University of Iasi, 11 Carol I, 700506 Iasi, Romania; alina.negru@uaic.ro

* Correspondence: carsene@uaic.ro; Tel.: +40-232-201354; Fax: +40-232-201313

Abstract: The Podu Iloaiei Dam Lake located on the Bahluet River from Bahlui hydrographic basin, north-eastern Romania, is one of the most important water resources used for aquaculture activities in the region of interest. In the present study, the chemical composition related to water-soluble ions and elements was assessed in both water and sediment samples collected from the area of interest during July 2017 and October 2017, representative months for warm and cold seasons, respectively. Water-soluble ions ($H_3C_2O_2^-$, HCO_2^-, $C_2O_4^{2-}$, F^-, Cl^-, NO_2^-, Br^-, NO_3^-, SO_4^{2-}, Li^+, Na^+, NH_4^+, K^+, and Ca^{2+}) were analyzed by ion chromatography, while inductively coupled plasma mass spectrometry was used to quantify water-soluble fractions of elements (Be, B, Mg, Al, Ti, V, Cr, Mn, Fe, Co, Ni, Cu, Zn, Ga, Ge, Rb, Sr, Mo, Ru, Pd, Ag, Cd, Sn, Sb, Te, Ba, Ir, Tl, Pb, Bi, and U). Evidence was obtained on the contributions of both anthropogenic and natural (pedologic) related sources in controlling the chemical composition of the water and sediment samples in the area. Analysis of Piper diagrams revealed the existence of CO_3^{2-}/HCO_3^- and Ca^{2+}/Mg^{2+} as dominant species for the sediment samples. The interest water pool was found to be oligotrophic over the warm period and eutrophic over the cold period. Overall, abundances and the association of chemical species in the area seemed to be controlled by a complex interplay between the water body's main characteristics, meteorological factors, and anthropogenic activities. Moreover, the present results suggest that precautions should be taken for physicochemical parameter monitoring and prevention acts for surface water quality assurance in order to control the potential negative influence of some chemical parameters on fish productivity. Reported data also have a high potential to be used by experts in the field of developing lake water management policies for a sustainable exploitation of various aquatic systems.

Keywords: heavy metals; water-soluble ions; spatial distribution; nutrients; Podu Iloaiei Dam Lake

check for updates

Citation: Amarandei, C.; Negru, A.-G.; Soroaga, L.-V.; Cucu-Man, S.-M.; Olariu, R.-I.; Arsene, C. Assessment of Surface Water Quality in the Podu Iloaiei Dam Lake (North-Eastern Romania): Potential Implications for Aquaculture Activities in the Area. *Water* **2021**, *13*, 2395. https://doi.org/10.3390/w13172395

Academic Editor: Aldo Fiori

Received: 30 July 2021
Accepted: 26 August 2021
Published: 31 August 2021

Publisher's Note: MDPI stays neutral with regard to jurisdictional claims in published maps and institutional affiliations.

Copyright: © 2021 by the authors. Licensee MDPI, Basel, Switzerland. This article is an open access article distributed under the terms and conditions of the Creative Commons Attribution (CC BY) license (https://creativecommons.org/licenses/by/4.0/).

1. Introduction

Changes in surface water's quality due to dramatically increased chemicals and nutrient materials threaten aquatic ecosystems and the environmental conditions. Evaluation of water and sediment physicochemical characteristics is highly important for quality control of surface water resources and for identification of potential exploitation. Safe water for fish farming requires water parameters to be in certain ranges [1], with some (e.g., pH, water hardness, etc.) being more difficult to be controlled in natural water reservoirs. Additionally, heavy metal contamination of the aquatic environment has drawn special attention because of the persistence, bioaccumulation, and potential adverse effects on biota [2]. Understanding the physicochemical parameters and evaluation of the anthropogenic impact on surface water and sediment are highly important for water quality

assessments and aquatic environmental protection. The sediment is a major sink of heavy metals due to scavenging of metals from the water column. However, it can also be a potential source of metal contamination into the water column and aquatic biota due to remobilization processes. The behavior of heavy metals in sediments, and therefore their distribution, is affected by changes in sediment grain size, organic content, and the redox regime [3]. The construction of dams on rivers and the loss of water discharge could cause the accumulation of anthropogenic waste in water reservoirs [4].

The water used for aquaculture purposes requires appropriate conditions to ensure fishes' growth (fish seeds, feed, fertilizers), and, along with the fish farming activities, chemical residues and microorganisms are usually produced as wastes [5]. Fertilizers are highly soluble substances frequently used for aquaculture purposes [6]. Most of these chemicals are well known for their potential to release nutrients that can cause eutrophication of natural waters. In aquaculture there are also other substances that are less frequently used. Among them, liming material, oxidants, disinfectants, osmoregulators, algicides, coagulants, herbicides, and probiotics should be mentioned [6]. Moreover, in aquaculture the ionic composition of water is important for fish hatching, feeding, development, larval growth, and survival [7]. The concentrations of Ca^{2+} and Mg^{2+} divalent cations play a very important role in the ionic regulation of freshwater fish, with both ions modulating the branchial permeability [8]. Water contamination with agricultural, industrial, or human waste could result in aquaculture product contamination and food safety concerns. However, nowadays there is an increased concern over the potential harm of aquaculture effluents on receiving water bodies and worries over the contamination of aquatic food products with bioaccumulative and potentially harmful chemicals [5,9]. At the European scale, waters' status and pressures are presented in Report No. 7/2018 of the European Environment Agency (EEA) [10]. The ecological status and potential of surface water bodies are assessed based on biological, physicochemical (nutrients, organic pollution, acidification), and hydromorphological elements. In terms of water quality, five classes, including high, good, moderate, poor, and bad, are usually referred to. When speaking about the chemical status derived from the evaluation of priority substances, waters can be assigned as "good" or "failing to achieve good." The EEA report indicates that, at the European scale, 38% of surface water bodies are in good chemical status, 46% are under the critical thresholds for this status, and 16% have an unknown status. Moreover, at the European level, just 40% of the surface water bodies are in good or high ecological status or potential.

The Podu Iloaiei water reservoir, located on the Bahluet River from the Bahlui River basin in north-eastern Romania, is one of the most important water resources used for aquaculture activities in the region of interest. It has both economic and socio-politic value since the area is considered as one of the most anthropized hydrological basins in the country. Anthropogenic activities have important implications for the formation and evolution of water resources in the Bahlui hydrological basin. Waste from the municipalities and farms located along the Bahluet River, agricultural runoff, the application of chemical fertilizers in agriculture, and transport routes around the reservoir are the potential pollution sources in the investigated area [11]. Nevertheless, little is known about the chemical parameter levels in the water and sediment of Podu Iloaiei Dam Lake.

Over the years, Directive 2000/60/EC [12] of the European Parliament and of the council establishing the framework for community action in the field of water policy have been implemented in Romania through the Ministry of Waters and Environmental Protection Order No. 161/2006 [13]. According to the norms for classification of surface water quality, the ecological status of water bodies is established on the base of five quality classes for surface waters (I–V) (Table S1 of the Supplementary Material).

For the Bahlui River basin, in terms of required parameters for establishing water quality class, only very few reports can be identified in the literature [14,15]. Both previous studies report measured values for chemical parameters limited to pH, CBO_5, CCO-Mn, NH_4^+, NO_2^-, NO_3^-, PO_4^{3-}, and Mg^{2+} [14,15]. There is also one study reporting about

the anthropogenic impact on urban soil properties from the Bahlui Floodplain [16]. The treatment station of the town of Targu Frumos and some livestock farms located along the Bahluet River are suggested as the main pollution sources of Podu Iloaiei Dam Lake [14]. The impact of anthropogenic activities on water quality parameters of glacial lakes from Rodnei mountains was also reported in a more recent study [17]. Relatively high concentrations of NH_4^+, NO_2^-, Ca, Mg, Fe, and Cu were identified even in this water representative for a more pristine environment.

Reports on the photochemistry induced either by hydroxyl or nitrite radicals in natural water samples collected from wells in the Letcani area (north-eastern Romania, Bahlui River basin) [18–21] or from selected Romanian lakes [22] are present in the literature. In some studies, the authors also report on experimental evidence for aromatic nitration upon irradiation of natural water samples since, in the interest zones, very high nitrate levels were identified [20,22,23]. However, other representative studies in Europe highlight fairly well the importance of surface water investigations [24].

In Romania, the governmental summary report from 2018 of the National Agency for Environmental Protection classifies the Podu Iloaiei Dam Lake water as moderate (class III) in terms of general physicochemical parameters, but no results are presented for specific pollutants and the chemical status [25]. In the present work, accurate concentrations of water-soluble ions and water-soluble elements in water and sediment samples from Podu Iloaiei Dam Lake were reported. The main objectives of the performed investigations were: (1) to determine the level of heavy metal and ion concentrations for evaluation of water quality status by seasonal change, (2) to investigate the spatial distributions of chemical parameters in water and sediment, (3) to identify their potential sources using the multivariate statistical analysis, and (4) to indicate the suitability of water quality for intensive fish farming purposes. Moreover, the work reported in the present study may be considered as a key reference point for further investigation on potential degradation processes of photolabile organic compounds or in identifying the role played by some elements, e.g., Fe, in the photoproduction of OH radicals under specific conditions.

2. Materials and Methods

2.1. Study Area and Sampling Strategy

The Podu Iloaiei Dam Lake is located in the north-eastern part of Romania (Figure 1) on the Bahluet River at a distance of 2.5 km upstream of the confluence with the Bahlui River, at 400 m upstream from the town of Podu Iloaiei, Iasi County. The Bahluet River is an affluent of the Bahlui River located in the area between the Moldavian Plain and the Central Moldavian Plateau. The average altitude of the hydrological basin is 159 m above sea level, and the multiannual average flow rate of Bahluet River is 1.06 m s^{-1} [26]. The main water input for Podu Iloaiei Dam Lake is Bahluiet River, and other sources include snow melting and natural springs. The Bahluiet River basin has a total surface of 550 km^2, a length of 50 km, an average slope of 13%, and a sinuosity coefficient of 1.23 [27].

The Podu Iloaiei Dam Lake was made to regulate the Bahluet River water flow rate, and it is used for fish farming and irrigation. Podu Iloaiei Dam Lake has a water surface of 251 ha and a dam of 14.1 m in elevation and 640 m in width [28]. The area and volume of Podu Iloaie Lake can vary considerably throughout the year. The water level is usually lower during the summer (June, July, and August) and higher during major rainfall events in the autumn (September, October, and November). The lake water is evacuated for the winter time.

The hydrographic basin is characterized by alluvial soils, carbonated alluviums, soils rich in sodium sulphates, meadow chernozem (formed on clayey and maroon substrates), and gray soils. Surface deposits are represented by monotonous succession of marches, clays, and sands with some intercalations of limestone sandstone, which is disposed monoclinally [11]. Bessarabia deposits (clay marls with intrusions of sand) from the Sarmatian age dominate the basin. Quaternary deposits from the Pleistocene age and Holocene deposits are also located in the Bahluet River area [27].

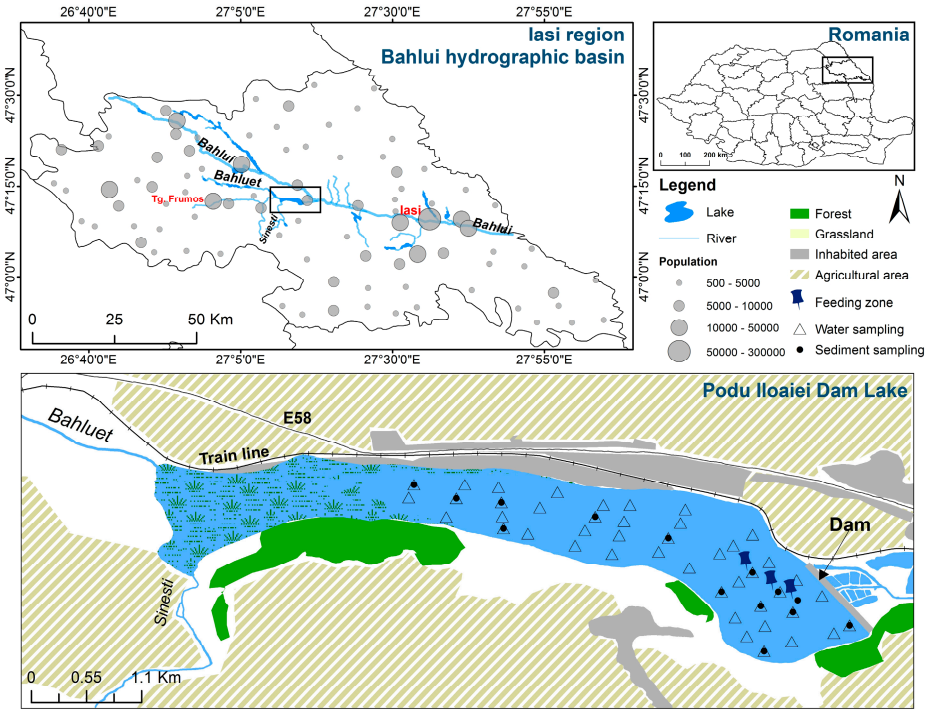

Figure 1. Location of the study area, water, and sediment sampling points.

The climate of the area is temperate–continental, with warm summers and cold winters. During the year, the temperature typically ranges from −5 °C to 28 °C, rarely reaching below −14 °C or above 33 °C, and the annual rainfall average is 589 mm. In the year the sampling was undertaken, May and June 2017 recorded the highest average precipitation values of 44 and 54 mm, respectively, and October 2017 was the month with the lowest rainfall, with an average of 27 mm.

According to the National Institute of Statistics, in the Prut–Barlad hydrographic area, including the Bahlui hydrographic area, about 71% of the surface is used for agriculture, 14% is covered by forests, 12% is occupied by construction, and 3% is occupied by surface waters [29]. The Podu Iloaiei Dam Lake is used for fish farming and is an important source of water for fishponds downstream of the dam [26].

In order to evaluate the chemical parameters of the investigated environment, water and sediment samples were collected from Podu Iloaiei Dam Lake in 50 mL polypropylene bottles in two sessions. The entire set of samples comprised 88 water samples and 28 sediment samples collected on 16 July 2017 and 5 October 2017, respectively. The sampling strategy was designed so as to obtain a significant number of data points for an accurate statistical treatment or for high-resolution distribution maps. The availability of technical resources was the limitative factor in increasing the sampling frequency or the number of the samples for each matrix. The distribution of the water and sediment sampling points is presented in Figure 1.

Water samples were collected from a ~10 cm depth (from the water surface layer), and sediment samples were collected from a ~20 cm depth (from the water–soil interface). The samples were stored at −4 °C until the analysis, which was performed within a maximum of 72 h after sampling.

2.2. Materials and Methods

2.2.1. Water-Soluble Ions Analysis by Ion Chromatography

The following inorganic anions: chloride (Cl^-), fluoride (F^-), bromide (Br^-), nitrite (NO_2^-), nitrate (NO_3^-), phosphate (PO_4^{3-}) and sulphate (SO_4^{2-}); organic anions: acetate ($H_3C_2O_2^-$), formate (HCO_2^-), and oxalate ($C_2O_4^{2-}$); and inorganic cations: sodium (Na^+),

potassium (K^+), lithium (Li^+), ammonium (NH_4^+), magnesium (Mg^{2+}), and calcium (Ca^{2+}) were quantified by ion chromatography.

The sediment samples were dried at 50 °C for 72 h in a ventilated oven (Ecocell), and 0.1–0.2 g of dry sediments were weighted and subjected to extraction with deionized water by ultrasound-assisted extraction (ultrasonic bath Elmasonic S70H, Elma, Singen, Germany) for 45 min at room temperature. The water samples and the aqueous extract of the sediment samples were filtered before analysis using cellulose acetate filters (ADVANTEC) with a pore diameter of 0.20 µm.

The ion determination was performed by the DIONEX ICS-5000+ DP system (Thermo Scientific, Waltham, MA, USA). In the case of anion determination, a 4.5/1.4 mM CO_3^{2-}/HCO_3^- solution was used for elution at a flow rate of 1.2 mL min^{-1}, using an AS22 column (4 × 250 mm) and an AERS 500 suppressor (4 mm). A 20 mM methanesulfonic acid solution was used as mobile phase at a flow rate of 1.0 mL min^{-1} for cation separation. In this case, a CS12A column (4 × 250 mm) and a CSRS 300 suppressor (4 mm) were used.

The external standard method was used to quantify water-soluble ions in both water and sediment samples. Calibration curves were performed in the concentration range of 50–3000 µg L^{-1} for anions and 50–2500 µg L^{-1} for cations. For the calibration curves, the required standard solutions were prepared by appropriate dilutions of seven anions-II and six cations-II Dionex standards. Calibration curves of water-soluble organic anions (acetate, formate, and oxalate) were acquired using solutions prepared with sodium salts of the anions (sodium acetate, ≥99%, from Merck, Darmstadt, Germany; sodium formate, 99%, and sodium oxalate, 99.9%, from AnalaR NORMAPUR, Leuven, Belgium).

The water samples' dilutions, the extraction of soluble ions from the sediment samples, and the preparation of the mobile phases and standard solutions were performed with deionized water (resistivity of 18.2 MΩ·cm) provided by the Milli-Q Advantage A10 system (Millipore, Burlington, MA, USA).

HCO_3^- is one of the major anions present in the water samples but cannot be determined by ion chromatography while using CO_3^{2-}/HCO_3^- as eluent. In an attempt to supplement the ionic balance, its estimation was used according to the method proposed by Arsene and co-workers [30]. The statistically significant correlation between the sum of the Ca^{2+} and Mg^{2+} concentrations and the anion deficit estimated from the ionic balance were taken into account. For both the sampling sessions, the linear regressions obtained between these variables are shown in Figure S1 of the Supplementary Material (SM).

2.2.2. Water-Soluble Elements Analyses by Inductively Coupled Plasma Mass Spectrometry

The analysis of water-soluble fractions of the elements in water and sediment samples was performed for Be, B, Mg, Al, Ti, V, Cr, Mn, Fe, Co, Ni, Cu, Zn, Ga, Ge, Rb, Sr, Mo, Ru, Pd, Ag, Cd, Sn, Sb, Te, Ba, Ir, Tl, Pb, Bi, and U by inductively coupled plasma mass spectrometry (ICP-MS) using the ICP-MS 7700X system (Agilent Technologies, Santa Clara, CA, USA). For the analysis, a 1 mL water sample and a 1 mL sediment aqueous extract (solution used for the ion chromatography analysis) were diluted with 8.5 mL 3% HNO_3. As an internal standard, 0.5 mL of indium (In) solution (1 mg L^{-1}) was added in each sample. Internal standard calibration curves were achieved using the multi-element standard solutions with 30 elements (Li, Be, B, Na, Mg, Al, K, Ca, V, Cr, Mn, Fe, Co, Ni, Cu, Zn, Ga, As, Se, Rb, Sr, Mo, Ag, Cd, Te, Ba, Tl, Pb, Bi, and U) and 8 elements (Ti, Ge, Mo, Ru, Pd, Sn, Sb, and Ir). Suprapur® nitric acid (65%) and all standard solutions used for ICP-MS analysis were purchased from Merck, Darmstadt, Germany.

During the analysis, in order to prevent the possible contributions brought by the contaminations, special emphasis was placed on carefully controlling the entire array of analysis steps. During the analysis sequence, for the quality control assurance, blanks and control samples were frequently analyzed. Tables S2 and S3 in the Supplementary Materials show the limits of detection (LoD) and the limits of quantification (LoQ) for the chemical species investigated in the present study.

2.3. Statistical Analysis of the Data

The mean, the standard deviation, and the median of the water-soluble ions and elements concentrations were calculated to obtain the variation between two different sampling sessions.

Multivariate statistical tools were applied in Origin 2018 to analyze the associations among different chemical species. Pearson's correlation coefficient and hierarchical cluster analysis were used for source apportionment. The Kolmogorov–Smirnov test was performed to check possible differences between the sampling sessions. Significant differences between the ions and the elements concentrations in both sampling sessions were identified with the value of $p < 0.05$ (95% confidence level).

Cluster analysis of the data with the Ward calculation method [31] was applied to identify possible common sources for the chemical species quantified in the water and sediment samples for both sampling sessions. This is a method of assessing the distance between two clusters by minimizing intra-cluster variability. Other studies in the field of water quality using the Ward method for cluster analysis have been identified in the literature [32,33]. Following the data processing, the graphs known as dendrograms show how the elements are grouped into classes according to the similarities between them.

The geostatistical method was implemented to comprehensively describe the variation of chemical species concentration in the surface water and sediment of Podu Iloaiei Dam Lake. In addition to the cluster analysis, the analysis of the geospatial distributions of the quantified species was used in order to discriminate between the potential contributions of the sources of pedological, atmospheric, or anthropogenic origin. In the literature, geostatistical data processing and the multivariate statistic data evaluation approach have been used for the investigation of pollutants in soil, sediment, and natural waters [34,35]. In order to achieve geospatial distributions of water-soluble ionic species quantified in water and sediment samples, the Google Earth Pro and ArcMap programs included in the ArcGIS 10.2 package were used. Kriging Ordinary interpolation methods with a spherical semivariogram and inverse distance weighting (IDW) interpolation were used for data processing. Compared to IDW, the Kriging method uses the theory of regionalized variables, which assumes that the direction and distance between data reflect a spatial correlation that is applied in explaining their variation by determining the semivariogram [36,37]. For this reason, the Kriging method is more complex and is not applicable to databases with a small number of cases. IDW is easier to apply, faster, not very restrictive in terms of the number of cases per variable or in terms of variance, and usually applies to highly variable data. The IDW method was used for sediment database comprised of a reduced number of available samples (14 compared to 44 for water).

3. Results

3.1. Water-Soluble Ions

The major ions quantified by ion chromatography in water and sediment samples were Cl^-, SO_4^{2-}, Mg^{2+}, Ca^{2+}, Na^+, and K^+. For ionic species quantified in water samples, excepting SO_4^{2-}, higher concentrations in samples collected in October were observed (Table 1). Figure S2 in the Supplementary Materials shows the linear regressions corresponding to the ionic balance for water and sediment samples including the estimated HCO_3^- contribution. For water samples (Figure S2a), compared to sediment samples (Figure S2b), an anion deficiency of 12% for samples collected in July and 18% for samples collected in October was observed. This could be associated with the presence of other organic compounds, such as amino acids and other carboxylic acids [38–41], that were not quantified in the present study.

Water hardness was calculated using the concentrations determined for Ca^{2+} and Mg^{2+} by ion chromatography (Table 1), and it was estimated as high as 352 ± 18 mg L^{-1} $CaCO_3$ in July and 412 ± 58 mg L^{-1} $CaCO_3$ in October. The values of electrical conductivity recorded in July and October were 474 ± 121 µS cm^{-1} and 956 ± 23 µS cm^{-1}, respectively.

Table 1. Water-soluble ions concentrations in water (mg L^{-1}) samples (n = 44), pH, conductivity (S, μS cm^{-1}), acid-neutralizing capacity (ANC, meq L^{-1}), and hardness (in mg L^{-1} $CaCO_3$) and water-soluble ions concentrations in sediment (μg g^{-1}) samples (n = 14) from Podu Iloaiei Dam Lake, north-eastern Romania. Data are presented as mean ± stdev (median) for the entire pool of analyzed samples (no flagged data).

Species/ Parameter	Water		Sediment	
	July	October	July	October
Cl^-	48.0 ± 5.2 (46.8)	63.0 ± 17.7 (57.6)	139 ± 39 (134)	94.7 ± 64.8 (74.7)
SO_4^{2-}	234 ± 7 (235)	181 ± 24 (179)	1121 ± 546 (1155)	1297 ± 484 (1170)
Na^+	153 ± 4 (152)	177± 9 (175)	476 ± 169 (513)	595 ± 195 (578)
K^+	13.6 ± 8.3 (10.4)	19.8 ± 15.3 (12.6)	284 ± 98 (294)	564 ± 133 (625)
Mg^{2+}	56.7 ± 1.6 (56.6)	62.9 ± 4.1 (62.7)	550 ± 139 (538)	1639 ± 320 (1728)
Ca^{2+}	47.5 ± 6.7 (45.6)	61.1 ± 17.8 (58.7)	1338 ± 692 (1179)	5041 ± 1350 (5305)
$N\text{-}NO_2^-$	0.40 ± 0.27 (0.40)	0.98 ± 1.12 (0.52)	28.0 ± 40.1 (11.4)	<1.86
$N\text{-}NO_3^-$	0.56 ± 0.42 (0.47)	1.56 ± 2.18 (0.92)	18.8 ± 26.4 (6.2)	7.92 ± 6.83 (8.29)
$N\text{-}NH_4^+$	0.65 ± 0.46 (0.55)	2.74 ± 1.67 (2.28)	142 ± 55 (138)	106 ± 70 (87)
$P\text{-}PO_4^{3-}$	<1.06	3.40 ± 2.20 (3.38)	17.0 ± 10.4 (11.5)	45.9 ± 16.7 (44.8)
$H_3C_2O_2^-$	32.5 ± 30.5 (24.1)	43.0 ± 43.0 (26.3)	394 ± 462 (230)	223 ± 118 (202)
HCO_2^-	4.27 ± 0.74 (4.27)	5.72 ± 6.57 (3.75)	91.1 ± 66.3 (63.6)	98.2 ± 47.4 (86.2)
$C_2O_4^{2-}$	<7.00	<7.00	64.0 ± 24.2 (60.3)	83.1 ± 35.9 (71.2)
pH	9.09 ± 0.15 (9.11)	8.25 ± 0.07 (8.24)		
S	474 ± 121 (491)	956 ± 23 (948)		
$CaCO_3$	366 ± 19 (349)	412 ± 58 (404)		
ANC	7.80 ± 0.52 (7.71)	10.8 ± 0.8 (10.6)		

F^-, Br^-, Li^+ species were below the LoD.

The investigated inorganic ions containing nitrogen or phosphorus were NO_2^- ($N\text{-}NO_2^-$), NO_3^- ($N\text{-}NO_3^-$), NH_4^+ ($N\text{-}NH_4^+$), and PO_4^{3-} ($P\text{-}PO_4^{3-}$). The $N\text{-}NH_4^+$ concentrations at the surface water level were 0.65 ± 0.46 mg L^{-1} in July and 2.74 ± 1.67 mg L^{-1} in October (Table 1). Oxalate could only be quantified in the water extracts of sediment samples, presenting lower concentrations than acetate and formate, 64.0 ± 24.2 μg g^{-1} compared to 394 ± 462 μg g^{-1} and 91.1 ± 66.3 μg g^{-1} in July, and 83.1 ± 35.9 μg g^{-1} compared to 222 ± 118 μg g^{-1} and 98.2 ± 47.4 μg g^{-1} in October (Table 1). $C_2O_4^{2-}$ is known to be an important component of plants [42]. It largely undergoes the process of bacterial decomposition with the formation of CO_2, but, in the case of hard water, $C_2O_4^{2-}$ precipitates in the form of CaC_2O_4 [43].

The water acid-neutralizing capacity (ANC) calculated with Equation (1) had the average values of 7.80 ± 0.52 meq L^{-1} in July and 10.8 ± 0.8 meq L^{-1} in October. These values indicate that the water is not susceptible to acidification. This aspect was confirmed by the pH measurements made in July and October, the mean values being 9.09 ± 0.15 and 8.25 ± 0.07, respectively.

$$ANC = ([Ca^{2+}] + [Mg^{2+}] + [Na^+] + [K^+]) - ([SO_4^{2-}] + [NO_3^-] + [Cl^-]) \quad (1)$$

3.2. Water-Soluble Elements

Table 2 shows the average concentrations of determined elements in water samples and aqueous sediment extracts for the interest sampling sessions. Higher concentrations of the quantified elements were observed for the October sampling session compared with the July sampling session.

The mean Cr concentration values were 0.019 ± 0.011 mg L^{-1} and 0.064 ± 0.048 mg L^{-1}, in July and October, respectively. The average values of Cr concentration (Table 2) classify the lake water in quality class II according to Order 161/2006 [13]. Variations in Cr concentrations in water can be associated with adsorption/desorption and precipitation/solubilization processes [44].

The average concentrations of Pb in water samples for both sampling sessions of 0.071 ± 0.062 mg L^{-1} and 0.078 ± 0.116 mg L^{-1} exceeded the limits of quality class IV (according to Order 161/2006), and a concentration of 0.025 mg L^{-1} was associated with

the waste water class. Measured concentrations of Ni and Mn in water samples collected in October were higher than the regulated values of 0.025 mg L^{-1} and 0.30 mg L^{-1}, respectively, corresponding to quality class IV.

Table 2. Averages of water-soluble elements' concentrations in water (mg L^{-1}, n = 44) and sediment (μg g^{-1}, n = 14) samples from Podu Iloaiei Dam Lake, north-eastern Romania. Data are presented as mean ± stdev (median).

Element	Water		Sediment	
	July	October	July	October
Al	1.00 ± 2.03 (0.48)	1.35 ± 1.70 (0.68)	96.5 ± 57.1 (79.6)	143 ± 80 (120)
Ti	<0.60	<0.60	8.67 ± 4.99 (7.60)	5.36 ± 4.93 (2.94)
Cr	0.019 ± 0.011 (0.019)	0.064 ± 0.048 (0.051)	1.21 ± 0.81 (0.79)	1.13 ± 0.80 (0.84)
Mn	0.097 ± 0.083 (0.072)	0.33 ± 0.21 (0.34)	20.0 ± 9.6 (18.7)	45.4 ± 26.9 (38.2)
Ni	0.12 ± 0.17 (0.09)	1.08 ± 3.04 (0.41)	14.4 ± 3.8 (14.2)	17.2 ± 5.3 (17.2)
Zn	0.79 ± 1.67 (0.12)	1.88 ± 2.52 (1.27)	15.3 ± 6.5 (17.7)	97 ± 161 (37)
Ge	0.14 ± 0.11 (0.13)	0.19 ± 0.13 (0.15)	19.6 ± 4.4 (20.3)	16.8 ± 4.1 (16.9)
Sr	0.54 ± 0.09 (0.52)	0.60 ± 0.42 (0.52)	10.6 ± 4.1 (9.4)	40.6 ± 11.5 (39.5)
Ag	0.075 ± 0.037 (0.073)	0.13 ± 0.10 (0.10)	0.61 ± 0.39 (0.45)	0.95 ± 0.75 (0.63)
Sb	0.006 ± 0.005 (0.005)	0.04 ± 0.06 (0.02)	0.26 ± 0.20 (0.18)	0.24 ± 0.13 (0.25)
Ba	0.059 ± 0.041 (0.054)	0.16 ± 0.14 (0.12)	22.1 ± 3.6 (21.7)	30.3 ± 8.3 (31.5)
Pb	0.071 ± 0.062 (0.062)	0.08 ± 0.12 (0.05)	1.93 ± 1.49 (1.52)	1.20 ± 1.99 (0.62)

Be, B, V, Fe, Co, Cu, Ga, Rb, Mo, Ru, Pd, Cd, Sn, Te, Ir, Tl, Bi, and U were below the LoQ.

4. Discussion

4.1. Water-Soluble Ions and Elements Related to Lake Water Typology

In both water and sediment samples the concentrations of the major ions collected in October were higher compared to July (Table 1). This was most likely the result of a significant contribution from the anthropogenic factors and less from the pedological factors or from the microbiological processes that naturally take place in the aquatic system. The Bahluet River supply water could be a source of waste for Podu Iloaiei Dam Lake because along its course fish farms, villages without sewerage, and agricultural lands are located. Differences between the two sampling seasons might also be due to the weather conditions during the collection time. In 2017, dilution of water-soluble ionic species and elements could occur in June and July due to more heavy raining events if compared to September and October. In water systems with a high-density fish population water quality can be altered by the chemicals added in order to maintain the parameters at an appropriate level. An increase in temperature, the consumption of oxygen by zooplankton, and the intensification of fodder residues' microbiological degradation processes may induce a critical decrease in dissolved oxygen. To prevent these, calcium hypochlorite ($Ca(ClO)_2$) is added to stabilize the amount of dissolved oxygen in the investigated system.

Figure 2 shows the percentage distributions of ionic species quantified in water (Figure 2a) and sediment (Figure 2b) samples and were calculated using the mean concentrations in meq L^{-1} for water and μeq g^{-1} (dry sediment) for sediment. From the percentage distributions presented in Figure 2, it was observed that for the water samples the major ions are present in the order $Na^+ > HCO_3^- > Mg^{2+} > SO_4^{2-} > Ca^{2+} > Cl^- > K^+$ and for the sediment samples $HCO_3^- > Ca^{2+} > Mg^{2+} > SO_4^{2-} > Na^+ > K^+ > Cl^-$. The dominant water anion was HCO_3^- followed by SO_4^{2-}. The high contributions of Na^+ (24.1%) and SO_4^{2-} (14.5%) ions can be associated with the pedological factor, the investigated area having characteristic saline soils with high levels of sodium sulphate [11]. An additional source of SO_4^{2-} could be represented by air pollution generated by rail transport (at ~250 m) and or by intense traffic on the road nearby.

Nitrogen and phosphorus are considered macronutrients, often limiting the development of phytoplankton. In the absence of nutrient pollution sources (fertilizers, wastewater rich in PO_4^{3-}, etc.), natural waters have low amounts of these species because there is a natural cycle that does not allow their accumulation in the environment. Unpolluted

natural surface waters have inorganic nitrogen concentrations of less than 0.01 mg L^{-1} N-NO_2^-, 0.2 mg L^{-1} N-NO_3^-, and 0.02 mg L^{-1} N-NH_4^+ [45]. Low levels of the dissolved oxygen in the water increase the anoxic processes at the water–sediment interface. Higher concentrations of N-NH_4^+ (Table 1) can be determined by biodegradation processes of organic matter under anoxic conditions. NO_2^- does not accumulate in the water because it is formed mainly as an intermediate in the nitrification process and has a low stability. Variations in the concentrations of P-PO_4^{3-}, N-NO_2^-, and N-NO_3^- could be attributed to local processes of organic matter biodegradation. For N-NH_4^+, the possibility of an anthropogenic source of contamination can be considered. A seasonal source for NH_4^+ could be the phytoplankton degradation in early autumn, local accumulations of organic matter being possible.

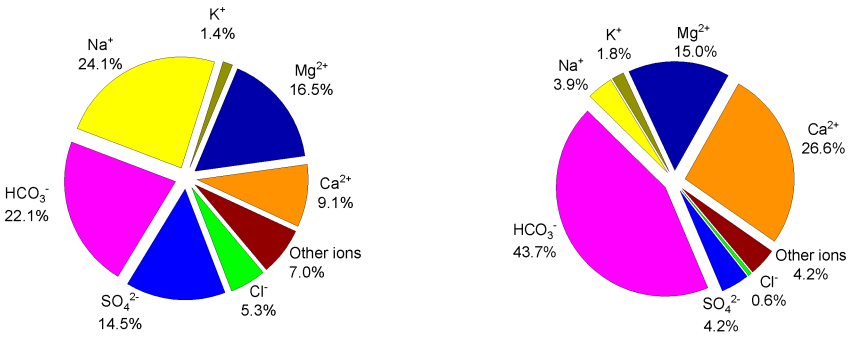

Figure 2. Relative concentration distribution of water-soluble ions quantified in water (**a**) and sediment (**b**) samples collected from Podu Iloaiei Dam Lake (other ions: $H_3C_2O_2^-$, HCO_2^-, $C_2O_4^{2-}$, PO_4^{3-}, NO_2^-, NO_3^-, NH_4^+).

In order to indicate the dominant typology of water, Piper diagrams were used. They allow the identification of water character by using the ratio of major ions. For water samples, the Piper diagram (Figure 3a) does not indicate the existence of a dominant water character, but the orientation towards $Na^+ + K^+$, $HCO_3^- + CO_3^{2-}$, and SO_4^{2-} can be observed. This could suggest the presence of Na^+, K^+, and SO_4^{2-} sources other than the solubilization process of sediment minerals, for example, the use of fertilizers in agriculture or the discharge of wastewater from households [6]. The difference between the diagrams can also be explained by the higher solubility of the Na^+ and K^+ salts compared to those of Mg^{2+} and Ca^{2+}. Additionally, among the major cations (Ca^{2+}, Mg^{2+}, K^+, Na^+), Ca^{2+} has the lowest hydrated ion radius that enhance its adsorption on the sediment. The physicochemical properties of the soil must be studied in order to explain the ion exchange processes that take place.

For sediment (Figure 3b) samples, a dominant character of Ca^{2+} (Mg^{2+}) HCO_3^- was observed. Higher concentrations of $Ca(HCO_3)_2$ and $CaCO_3$ in samples collected in October compared to July could be determined by the increase in the solubility of these species when the temperature decreases, a phenomenon considered in other study [46].

Both for water (Figure 4a) and sediment (Figure 4b) samples, important variations were observed between the sampling periods for most of the elements' concentrations. These could indicate a waste accumulation in the water and sediment due to the Bahluet River contributions and fish food addition. The variations could indicate the presence of temporary pollution sources such as waste discharge and secondary pollution sources represented by the selective mobilization of metals from sediment enhanced by higher major ions concentrations in the samples collected in October compared to July.

As previously presented, the Podu Iloaiei Dam Lake water is characterized by a high content of major ions. Acosta and co-workers [47] highlighted the mobilization of Pb enhanced by an increase in $CaCl_2$, $MgCl_2$, NaCl, and Na_2SO_4 salinity. These could be

determined by the high concentrations of major ions, especially Ca^{2+}, Mg^{2+}, Na^{+}, which can lead to the mobilization of heavy metals from the sediment by the ion exchange process [2].

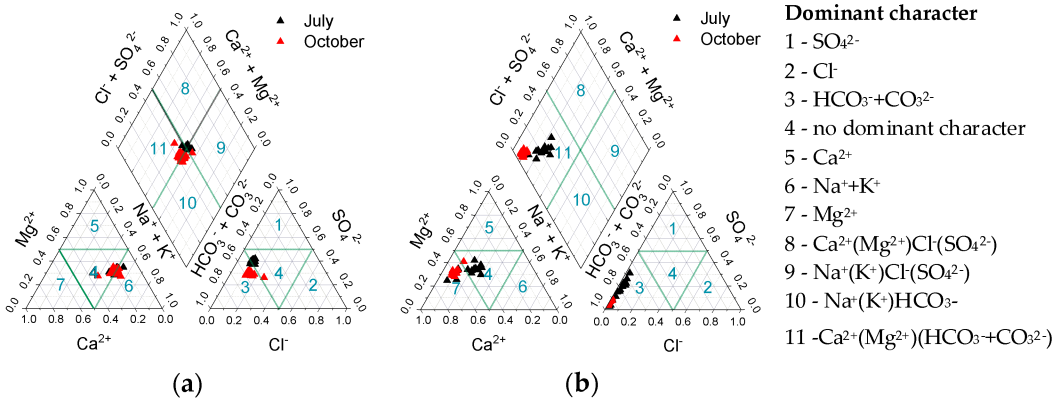

Figure 3. Piper diagrams corresponding to water (**a**) and sediment (**b**) samples collected from Podu Iloaiei Dam Lake.

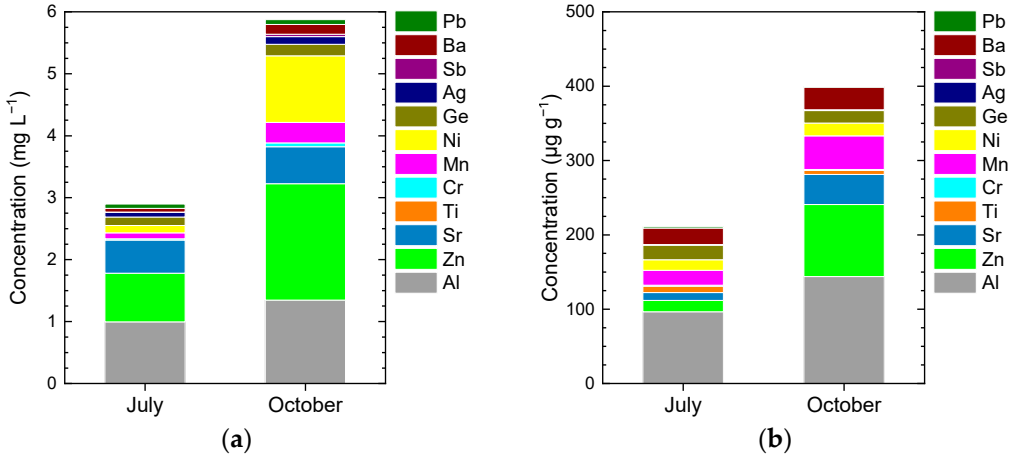

Figure 4. The cumulative concentrations of the water-soluble elements quantified in water (**a**) and sediment (**b**) samples collected from Podu Iloaiei Dam Lake in each sampling session.

4.2. Distribution of Chemical Parameters in the Podu Iloaiei Dam Lake

The dendrograms obtained by the Ward method for selected species quantified in water and sediment samples collected in both July and October sampling sessions are presented in Figure 5. Prior to this analysis, the data were normalized. The distribution of chemical species within the clusters suggests that Sr, Mg^{2+}, Cl^{-}, SO_4^{2-}, Na^{+}, and Ca^{2+} can be associated with the pedological factor. The association is highlighted by the Pearson's correlation coefficient values calculated and presented in Tables S4 and S5 in the Supplementary Materials. Natural contributions for these species could be soil runoff and mobilization of soluble species in water from the sediment and soil.

For the water samples (Figure 5a), a cluster including Al, Zn, Pb, NH_4^{+}, and K^{+} was highlighted, indicating fish food administration as a possible source for these species. A common source for NH_4^{+} and K^{+} could be the use of fertilizers in agriculture and the bacterial degradation of plant residues rich in organic compounds with N and K^{+}. The Sb, Ti, Ge, Ba, Mn, Cr, Zn, and Ag determined in sediment were grouped in one cluster, suggesting that the main contribution for these elements could be attributed to the pedological factor. A strong association between Pb and Al in sediment could indicate their anthropogenic origin. Additionally, a statistically significant correlation factor of 0.77 ($p < 0.001$) (Table S5 in the Supplementary Materials) between these elements was observed.

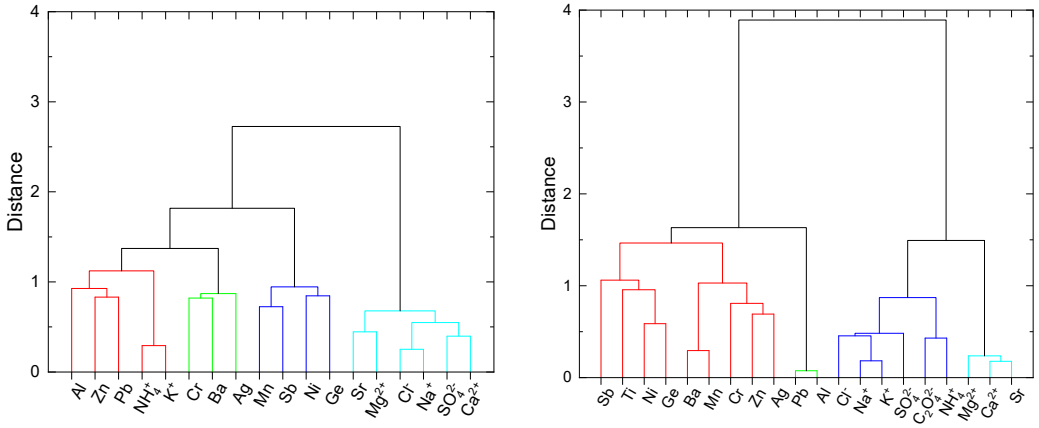

Figure 5. Hierarchical dendrograms showing clustering of water-soluble ions and elements in water (**a**) and sediment (**b**) samples collected in July and October sampling sessions.

Geospatial distributions in the water samples of the pH and conductivity parameters, beside those of water-soluble ions as Mg^{2+}, Ca^{2+}, NH_4^+, Na^+, SO_4^{2-}, Cl^-, and NO_3^-, are shown in Figure 6. Figure S3 of the Supplementary Materials presents the geospatial distributions of K^+, NO_2^-, $H_3C_2O_2^-$, and HCO_2^- concentrations in both water and sediment samples. There was a clear discrimination between areas with two different particularities in terms of potential existent acidity and alkaline driven species. From Figure 6 it is clearly observed that water-soluble Mg^{2+}, Ca^{2+}, and NH_4^+ are major ionic species controlling alkalinity. While over the July session, the NH_4^+ species seemed to play an important role in the area where the water depth was lower, in the October session, it was obvious that the importance of this ion in controlling water pH might enhance in the feeding area. The values of the pH parameter measured for both July and October sessions allow us to suggest the potential transition of NH_4^+ to the toxic and volatile NH_3, which might occur in the investigated water lake.

In water samples, several common point sources are easily identified in the geospatial distributions of Ca^{2+}, Cl^-, and NO_3^- (Figure 6). Areas with higher conductivity (Figure 6) correspond to areas with higher Mg^{2+}, NH_4^+ (Figure 6), and K^+ (Figure S3 in the Supplementary Materials) concentrations.

Figure 7 shows the distribution of Mg^{2+}, Ca^{2+}, NH_4^+, Na^+, SO_4^{2-}, Cl^-, NO_3^-, and $C_2O_4^{2-}$ in sediment samples. Similar geospatial distributions of Mg^{2+}, Ca^{2+}, Na^+, SO_4^{2-} (Figure 6), and K^+ (Figure S3 in the Supplementary Materials) concentrations were observed. $C_2O_4^{2-}$ was quantified only in sediment samples with higher concentration values in the feeding area (Figure 6). Since the investigated water lake is assigned as hard water, $C_2O_4^{2-}$ is most probably present as a precipitate in the form of CaC_2O_4.

The spatial distributions for the elements Sr, Cr, Pb, Mn, Zn, Ba, Ni, and Sb in the water and sediment samples collected from Podu Iloaiei Dam Lake are presented in Figures 8 and 9, while Figure S4 of the Supplementary Materials shows the distributions of Al, Ge, and Ag. The Sr concentration variations in the sediment (Figure 9) present a similar profile with Mg^{2+}, Ca^{2+}, Na^+, and SO_4^{2-} (Figure 6). In the south-eastern part of the lake, at the lateral end of the dam, in both sampling sessions, a spot corresponding to high concentrations for Cr, Pb, Mn, Zn, Ba, Ni (Figures 8 and 9), and Al (Figure S4 in the Supplementary Materials) was observed, indicating the existence of a punctual and persistent source of pollution. Geospatial distributions describe different areas with high and low concentrations for Cr and Pb in water (Figure 6) and sediment (Figure 7) samples. These highlight different sources or mobilization processes for these elements. For water samples collected in October, an increase in Mg^{2+} (Figure 6), K^+ (Figure S3 in the Supplementary Materials), Mn, and Zn (Figure 8) concentrations was observed in the feeding area, possibly generated by the fish food addition.

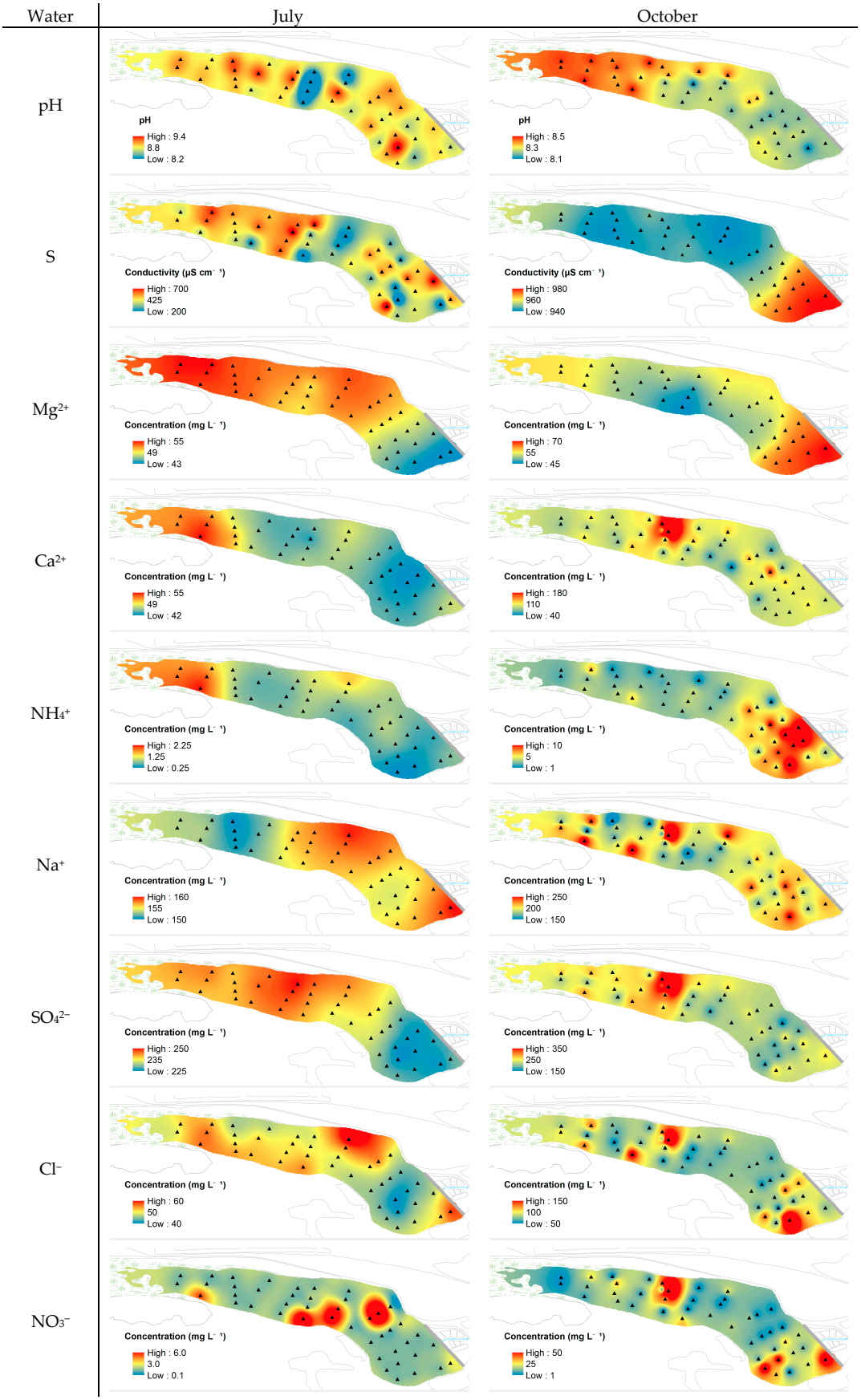

Figure 6. Spatial distribution of pH, conductivity (S), Mg^{2+}, Ca^{2+}, NH_4^+, Na^+, SO_4^{2-}, Cl^-, and NO_3^- in water of Podu Iloaiei Dam Lake for July and October sampling sessions.

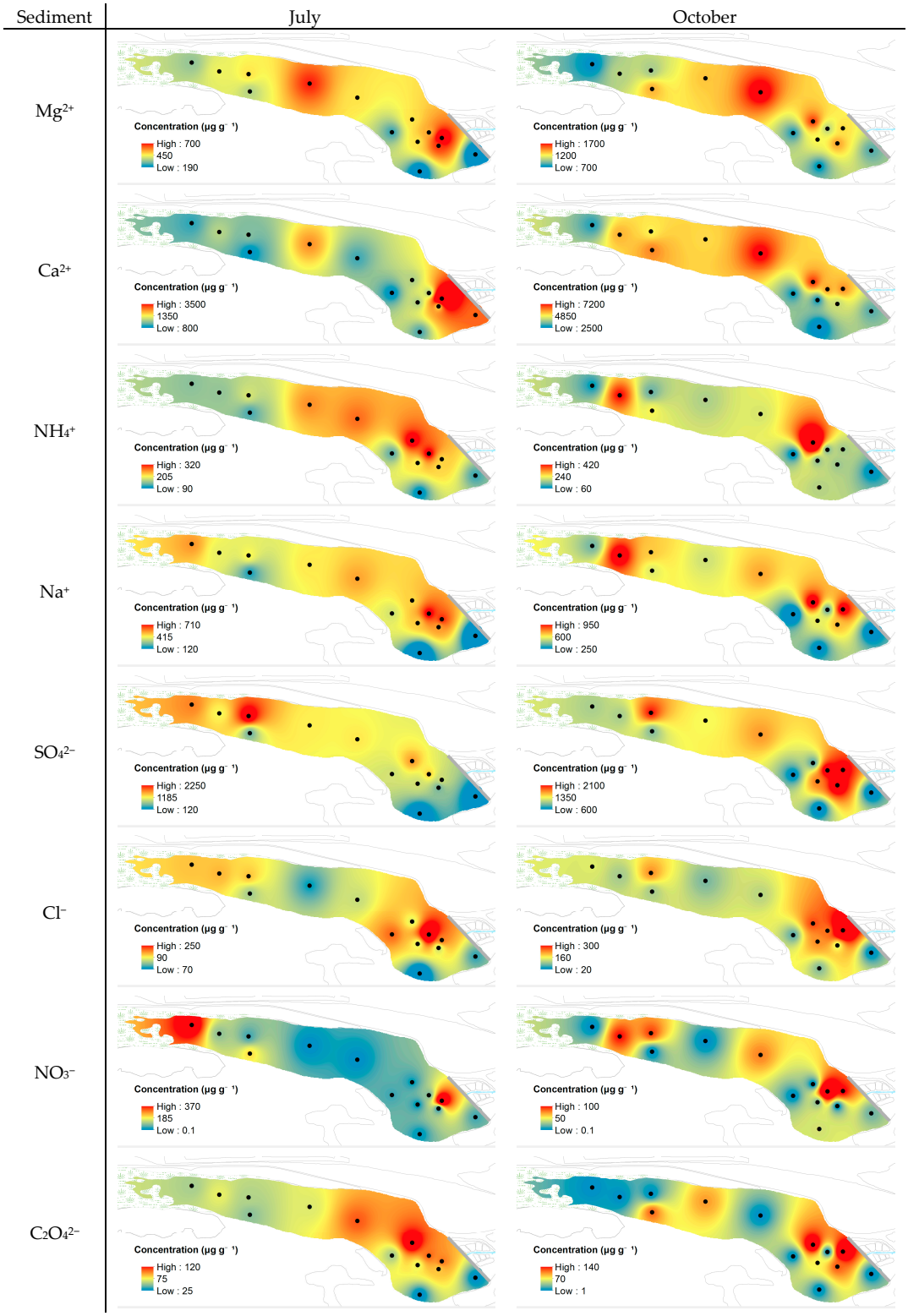

Figure 7. Spatial distribution of Mg^{2+}, Ca^{2+}, NH_4^+, Na^+, SO_4^{2-}, Cl^-, NO_3^-, and $C_2O_4^{2-}$ in sediment of Podu Iloaiei Dam Lake for July and October sampling sessions.

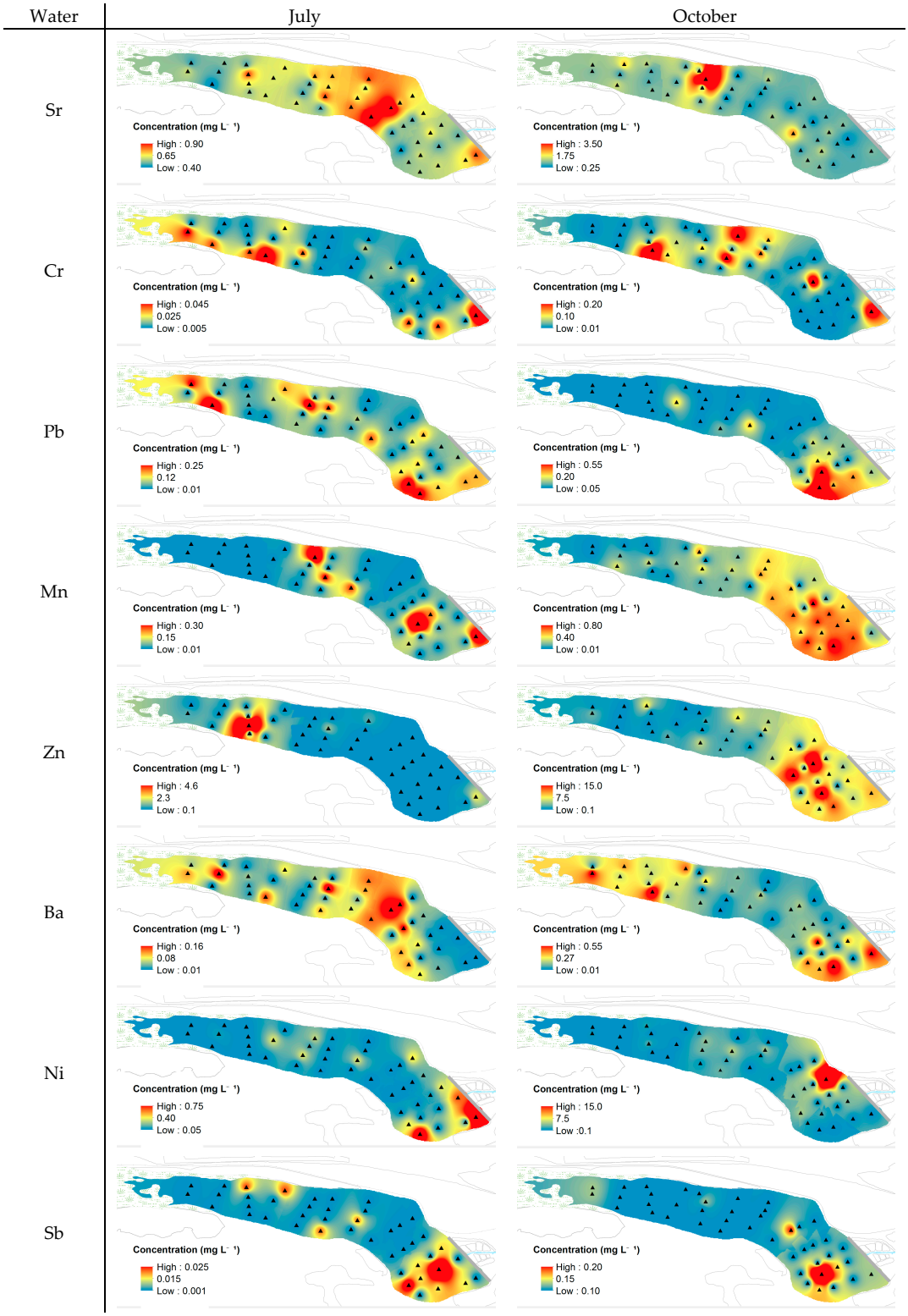

Figure 8. Spatial distribution of Sr, Cr, Pb, Mn, Zn, Ba, Ni, and Sb in water of Podu Iloaiei Dam Lake for July and October sampling sessions.

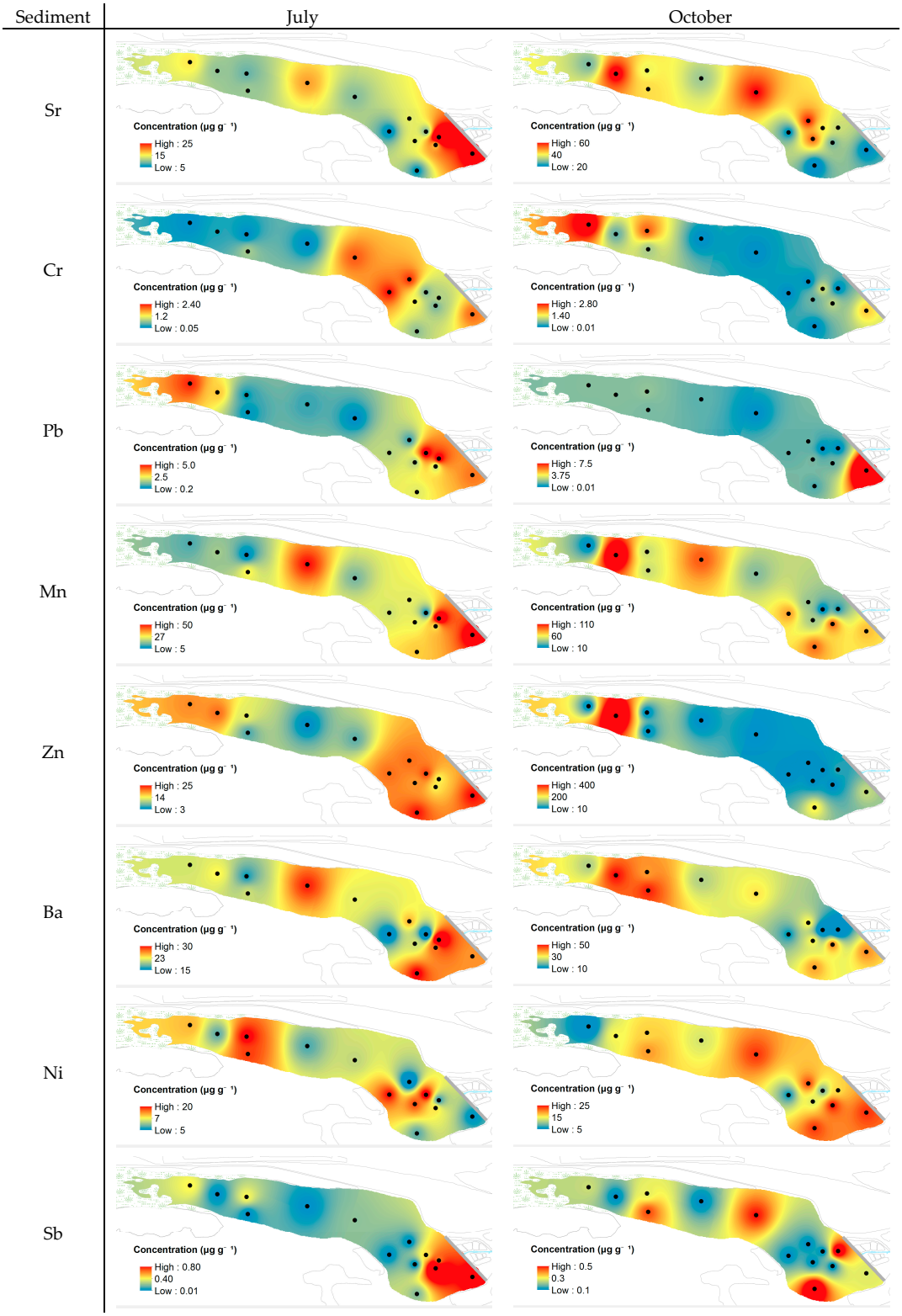

Figure 9. Spatial distribution of Sr, Cr, Pb, Mn, Zn, Ba, Ni, and Sb in sediment of Podu Iloaiei Dam Lake for July and October sampling sessions.

The Kolmogorov–Smirnov test applied to the database indicated significant different distributions of Cr, Mn, Ni, Zn, Sb, Ba, Cl^-, SO_4^{2-}, Na^+, NH_4^+, K^+, Mg^{2+}, and Ca^{2+} concentrations. For Al, Ge, Sr, Ag, and Pb present in water samples collected in different sampling sessions from Podu Iloaiei Dam Lake the differences were not significant. Additionally,

significant different concentrations were observed for Al, Ti, Mn, Sr, Ag, Ba, Pb, Cl^-, K^+, Mg^{2+}, and Ca^{2+}, while insignificant differences were noticed for Cr, Ni, Zn, Ge, Ag, Sb, SO_4^{2-}, $C_2O_4^{2-}$, Na^+, and NH_4^+ in sediment samples collected in both seasons from the investigated water.

4.3. Suitability of the Podu Iloaei Lake for Aquaculture Purposes and Potential Practical Implications

Water quality is one of the main concerns in aquaculture [9]. Changes in the chemical or physical parameters can cause negative effects on the growth of the aquatic organisms, their physiological state, or even mortality, with major losses in production.

The physicochemical parameters measured in small-scale fish production systems are pH, conductivity, and dissolved oxygen. Elements' presence or other ions in water sources are not generally measured. Besides the water source, the quality of the effluent water is highly important when considering environmental aspects of fish production. Aquaculture's increase over the last years could have an important impact on the environment and natural water resources. Some concerns include: water pollution resulting from pond effluents (i.e., salinization of water by effluents, seepage, and sediment), excessive use of ground water and other freshwater sources to increase the water level in ponds, the spread of aquatic animal diseases from cultured organisms to native populations, and negative effects on biodiversity caused by the escape of non-native species introduced for aquaculture [9].

The lake water (Podu Iloaiei Dam Lake) investigated in the present study had a hardness higher than 180 mg L^{-1} $CaCO_3$, and therefore it was considered a very hard water. Waters with a hardness higher than 300 mg L^{-1} $CaCO_3$ do not provide optimal conditions for high fish productivity [7]. It is recommended that the pH of the water be in the 7.0–8.5 range because fish blood has an average pH of 7.4 [1]. The pH values measured in the present work over both the July and October sampling sessions allowed us to suggest that precautions be taken by the Podu Iloaiei Dam Lake administrator in order to prevent the potential negative influence of increased alkalinity on fish productivity.

Moreover, attention should be given to the water status in full compliance with the requirements derived from the National Agency for Environmental Protection Report on the state of the environment in the Iasi County [25]. The report clearly shows that from six dam lakes located in the Prut basin, five lakes did not meet the moderate ecologic potential (Class III) [25]. However, while in the report from 2018, the Podu Iloaiei Dam Lake was classified as moderate with no traceable measurements for specific chemical parameters [25], in the report covering measurements from 1997 to 2004, the lake water was included either in class IV (pH, CBO_5, CCO-Mn, NH_4^+, Mg^{2+}) or in class III (NO_2^-, NO_3^-, PO_4^{3-}) [14] of quality. Considering the total nitrogen and phosphorus levels reported in 2014 [15] the water lake was assigned as hypertrophic.

In the present study, according to the classification of waters in the quality classes, used to establish the ecological status of water bodies [13], the Podu Iloaiei Dam Lake water falls in water quality class III based on the SO_4^{2-}, Na^+, Mg^{2+} and nutrient contents. This suggests that Podu Iloaiei Dam Lake can be suitable for aquaculture, but it is not recommended to breed fish species sensitive to high hardness and high ionic strength because they can suffer imbalances at the osmoregulatory system level. The productivity could also be reduced due to the difficulty of nutrient adsorption in such conditions [7]. Higher concentrations of water-soluble ions in October could indicate an increase in dissolved solids, which has the effect of decreasing the gases' solubility in water, which can also negatively affect the osmotic balance of fish [48].

Considering the trophicity classes proposed by Dodds and co-researchers [49], with regard to nutrient concentration limits, the Podu Iloaiei Dam Lake water has an oligotrophic character in July, while, in October, the nutrient level corresponds to the eutrophic waters. Factors that could cause this variation are the discharge of waste waters, the administration of fertilizers in the agricultural area, the administration of fish food, and low rainfall that implied reduced discharge in order to keep the optimal level of water.

From the investigated elements, Pb seems to be highly influenced by the anthropogenic factor, considering that the average concentration of Pb in water samples exceeded the limits for the quality class IV associated with the waste water category.

Overall, the Podu Iloaiei Dam Lake seems to have chemical characteristics of a system controlled by both natural and anthropogenic origin sources. A complete database in terms of common chemical parameters; chemical pollutants; parameters representative for aquaculture activities, such as dissolved oxygen, biological oxygen demand, and chemical oxygen demand; and potential chemical processing of the specific water system would be of great benefit for the administration of such water resources in order to develop appropriate planning and lake exploitation. Moreover, such information might be used by experts in the field of developing lake management policies for a sustainable exploitation of various aquatic systems.

5. Conclusions

Water and sediment samples from Podu Iloaiei Dam Lake located on the Bahluet River from the Bahlui hydrographic basin, north-eastern Romania, were investigated in order to determine their chemical composition in terms of the water-soluble constituents.

Anthropogenic and natural (pedologic) related sources seem to control the chemical composition of the water and sediment samples in the area. Experimental evidence obtained within the present work allowed us to infer that the Podu Iloaiei Dam Lake water was not susceptible to acidification. The trophicity of the investigated lake water seemed to present seasonal variability, changing from oligotrophic during warm periods to eutrophic over cold periods. Moreover, the Podu Iloaiei Dam Lake water traces the characteristics of a potential saline soil existent in the nearby region. The abundance of water-soluble chemical species suggests not only the solubilization process of sediment minerals but also the use of fertilizers in agriculture as important sources in the water body of interest. Uncontrolled or accidental waste discharge and secondary pollution sources might have contributions to the water characteristics.

The complex interplay between the water body's main characteristics, meteorological factors, and anthropogenic activities in the area control the abundances and the association of chemical species present in the water body. The results of the present study allow us to suggest that the Podu Iloaiei Dam Lake is suitable for aquaculture activities, but it is not recommended to breed fish species sensitive to high hardness and high ionic strength because they can suffer imbalances at the osmoregulatory system level.

The present study reports on the investigation of chemical parameters that are not routinely monitored at the European scale but which might have relevance for further studies concerning photochemical processing or when investigating health issues related to the consumption of aquaculture products exposed to potential toxics. However, due to various sources of water pollution, further studies might also evaluate and consider other important parameters such as dissolved oxygen, biological oxygen demand, and chemical oxygen demand as indicators for pollution. Moreover, further research could also involve measurements of physicochemical parameters in other water bodies (e.g., Bahluet River) in the region of interest. The evaluation of different water chemical treatments' impact on fish farming productivity and water quality in the Bahlui hydrographic basin might also be of interest.

Supplementary Materials: The following are available online at https://www.mdpi.com/article/10.3390/w13172395/s1, Table S1: Classification of waters in the quality classes in order to establish the ecological status of water bodies (extracted from Order no. 161/2006), Table S2: Limits of detection (LoD) and limits of quantification (LoQ) for ion chromatography determined water-soluble ions in the water and sediment samples, Table S3: Limits of detection (LoD) and limits of quantification (LoQ) for inductively coupled plasma mass spectrometry determined elements in the water and sediment samples, Table S4: Pearson's correlation coefficient of chemical species, pH, and conductivity (S) determined in water samples collected from Podu Iloaiei Dam Lake, Table S5: Pearson's correlation coefficient of chemical species quantified in sediment samples collected from Podu Iloaiei Dam Lake,

Figure S1: Linear regression between (∑cations − ∑identified anions) and ($[Mg^{2+}]$ + $[Ca^{2+}]$) for water samples (a) and sediment (b) samples in both sampling sessions, Figure S2: Linear regression for the ionic balance evaluation of water (a) and sediment (b) samples (including the HCO^{3-} estimation), Figure S3: Spatial distribution of K^{+}, NO^{2-}, $H_3C_2O^{2-}$, and HCO^{2-} in water and sediment of Podu Iloaiei Dam Lake, Figure S4: Spatial distribution of water-soluble Al, Ge, Ag, and Sb in water and sediment of Podu Iloaiei Dam Lake.

Author Contributions: Conceptualization, C.A. (Cornelia Amarandei), S.-M.C.-M., R.-I.O., and C.A. (Cecilia Arsene); methodology, C.A. (Cornelia Amarandei), R.-I.O., and C.A. (Cecilia Arsene); methods validation, C.A. (Cornelia Amarandei), A.-G.N., and L.-V.S.; formal analysis, C.A. (Cornelia Amarandei), A.-G.N., L.-V.S., S.-M.C.-M., R.-I.O., and C.A. (Cecilia Arsene); investigation, C.A. (Cornelia Amarandei), A.-G.N., L.-V.S., S.-M.C.-M., R.-I.O., and C.A. (Cecilia Arsene); resources, S.-M.C.-M., R.-I.O., and C.A. (Cecilia Arsene); data curation, C.A. (Cornelia Amarandei), A.-G.N., L.-V.S., S.-M.C.-M., R.-I.O., and C.A. (Cecilia Arsene); writing—original draft preparation, C.A. (Cornelia Amarandei); writing—review and editing, A.-G.N., L.-V.S., S.-M.C.-M., R.-I.O., and C.A. (Cecilia Arsene); supervision, C.A. (Cecilia Arsene). All authors have read and agreed to the published version of the manuscript.

Funding: This research received no external funding.

Data Availability Statement: Data are available upon request to the contact author Cecilia Arsene (carsene@uaic.ro).

Acknowledgments: The authors express their gratitude to the Administration of the Podu Iloaiei Dam Lake for facilitating access in the area for sampling purposes. Acknowledgment is given by S.-M.C.-M., R.-I.O., and C.A. (Cecilia Arsene) to the infrastructure support from the Operational Program Competitiveness 2014–2020, Axis 1, under POC/448/1/1 research infrastructure projects for public R&D institutions/Sections F 2018, through the Research Center with Integrated Techniques for Atmospheric Aerosol Investigation in Romania (RECENT AIR) project, under grant agreement MySMIS no. 127324. Acknowledgments are given to the CNFIS-FDI-2021-0501 project as well.

Conflicts of Interest: The authors declare no conflict of interest.

References

1. Wurts, W.A.; Durborow, R.M. *Southern Regional Aquaculture Center Interactions of pH, Carbon Dioxide, Alkalinity and Hardness in Fish Ponds*; SRAC Publication No. 464; Southern Regional Aquaculture Center: Stoneville, MI, USA, 1992.
2. Schuler, M.S.; Relyea, R.A. A Review of the Combined Threats of Road Salts and Heavy Metals to Freshwater Systems. *Bioscience* **2018**, *68*, 327–335. [CrossRef]
3. Kalantzi, I.; Shimmield, T.M.; Pergantis, S.A.; Papageorgiou, N.; Black, K.D.; Karakassis, I. Heavy metals, trace elements and sediment geochemistry at four Mediterranean fish farms. *Sci. Total Environ.* **2013**, *444*, 128–137. [CrossRef] [PubMed]
4. Palanques, A.; Grimalt, J.; Belzunces, M.; Estrada, F.; Puig, P.; Guillén, J. Massive accumulation of highly polluted sedimentary deposits by river damming. *Sci. Total Environ.* **2014**, *497–498*, 369–381. [CrossRef]
5. Ahmad, A.; Sheikh Abdullah, S.R.; Hasan, H.A.; Othman, A.R.; Ismail, N. Izzati Aquaculture industry: Supply and demand, best practices, effluent and its current issues and treatment technology. *J. Environ. Manag.* **2021**, *287*, 112271. [CrossRef] [PubMed]
6. Boyd, C.E.; Massaut, L. Risks associated with the use of chemicals in pond aquaculture. *Aquac. Eng.* **1999**, *20*, 113–132. [CrossRef]
7. Luo, S.; Wu, B.; Xiong, X.; Wang, J. Effects of total hardness and calcium: Magnesium ratio of water during early stages of rare minnows (*Gobiocypris rarus*). *Comp. Med.* **2016**, *66*, 181–187.
8. Wendelaar Bonga, S.E.; Löwik, C.J.M.; van der Meij, J.C.A. Effects of external Mg^{2+} and Ca^{2+} on branchial osmotic water permeabiligy and prolactin secretion in the teleost fish Sarotherodon mossambicus. *Gen. Comp. Endocrinol.* **1983**, *52*, 222–231. [CrossRef]
9. Boyd, C.E. Guidelines for aquaculture effluent management at the farm-level. *Aquaculture* **2003**, *226*, 101–112. [CrossRef]
10. European Environment Agency. *European Waters. Assessment of Status and Pressures 2018*; European Environment Agency: Copenhagen, Denmark, 2018; ISBN 1977-8449.
11. National Administration "Romanian Waters" Prut-Barlad Water Basin Administration, Annual Report 2016. Available online: http://prut-barlad.rowater.ro/wp-content/uploads/2021/07/Raport-activitate-2016.pdf (accessed on 25 July 2021).
12. European Commission. Directive 2000/60/EC of the European Parliament and of the Council of 23 October 2000 establishing a framework for community action in the field of water policy. *Off. J. Eur. Communities* **2000**, *327*, 1–73.
13. Ministry of Environment and Water Management. The Norm Regarding the Classification of Surface Water Quality in Order to Establish the Ecological Status of Water Bodies; Published in the Official Monitor no. 511 Bis of June 13, 2006, Approved by Order no. 161 of 16.02.2006 2006. Available online: http://legislatie.just.ro/Public/DetaliiDocumentAfis/74255 (accessed on 25 July 2021).

14. Minea, I. The Evaluation of The Water Chemistry and Quality for The Lakes from the South of the Hilly Plain of Jijia (Bahlui Drainage Basin). *Lakes Reserv. Ponds* **2010**, *4*, 131–144.
15. Popoiu, L.A. Cercetări Privind Calitatea Apelor din Lacurile de Acumulare Mici și Mijlocii din Zonele Colinare. Ph.D. Thesis, Gheorghe Asachi Technical University of Iași, Iași, Romania, 2017.
16. Secu, C.V.; Breaban, I.G.; Juravle, D.T.; Lesenciuc, C.D. Human impact on urban soil properties from Bahlui Foodplain, Iasi, Romania. *J. Environ. Prot. Ecol.* **2016**, *17*, 154–163.
17. Roșca, O.M.; Dippong, T.; Marian, M.; Mihali, C.; Mihalescu, L.; Hoaghia, M.A.; Jelea, M. Impact of anthropogenic activities on water quality parameters of glacial lakes from Rodnei mountains, Romania. *Environ. Res.* **2020**, *182*, 109–136. [CrossRef] [PubMed]
18. Vione, D.; Falletti, G.; Maurino, V.; Minero, C.; Pelizzetti, E.; Malandrino, M.; Ajassa, R.; Olariu, R.I.; Arsene, C. Sources and sinks of hydroxyl radicals upon irradiation of natural water samples. *Environ. Sci. Technol.* **2006**, *40*, 3775–3781. [CrossRef]
19. Vione, D.; Ravizzoli, B.; Rinaldi, E.; Pettinato, F.; Arsene, C.; Olariu, R.I. Studies regarding groundwater quality at rural sites: 1. Estimation of the anthropic factor impact by complementary chemical analyses. *Rev. Chim.* **2009**, *60*, 237–240.
20. Vione, D.; Rinaldi, E.; Minero, C.; Maurino, V.; Olariu, R.I.; Arsene, C. Studies regarding groundwater quality at rural sites. 2. Photochemical generation of OH and NO2 radicals upon UV-A irradiation of nitrate-rich groundwater. *Rev. Chim.* **2009**, *60*, 551–554.
21. Vione, D.; Lauri, V.; Minero, C.; Maurino, V.; Malandrino, M.; Carlotti, M.E.; Olariu, R.I.; Arsene, C. Photostability and photolability of dissolved organic matter upon irradiation of natural water samples under simulated sunlight. *Aquat. Sci.* **2009**, *71*, 34–45. [CrossRef]
22. Vione, D.; Casanova, I.; Minero, C.; Duncianu, M.; Olariu, R.I.; Arsene, C. Assessing the potentiality of Romanian surface waters to produce hydroxyl and nitrite radicals. *Rev. Chim.* **2009**, *60*, 123–126.
23. Vione, D.; Khanra, S.; Man, S.C.; Maddigapu, P.R.; Das, R.; Arsene, C.; Olariu, R.I.; Maurino, V.; Minero, C. Inhibition vs. enhancement of the nitrate-induced phototransformation of organic substrates by the •OH scavengers bicarbonate and carbonate. *Water Res.* **2009**, *43*, 4718–4728. [CrossRef]
24. Diamantini, E.; Lutz, S.R.; Mallucci, S.; Majone, B.; Merz, R.; Bellin, A. Driver detection of water quality trends in three large European river basins. *Sci. Total Environ.* **2018**, *612*, 49–62. [CrossRef]
25. National Agency for Environmental Protection. *Report on the State of the Environment in Iasi County for 2018*. Available online: http://www.anpm.ro/documents/839616/2486913/raport+anual+20181.pdf/7ca6f7fa-5823-4214-8c9e-a19d6fb88466 (accessed on 24 July 2021).
26. WATER PIN Limited Liability Company. *Securing the Podu Iloaiei Reservoir, on the Bahluet River, Iasi County, Synthesis Memoir*. 2011. Available online: https://www.scribd.com/document/375298910/Memoriu-de-Sinteza-Ac-Podu-Iloaiei (accessed on 23 July 2021).
27. Nicu, C.I.; Asandulesei, A. GIS-based evaluation of diagnostic areas in landslide susceptibility analysis of Bahluieț River Basin (Moldavian Plateau NE Romania). Are Neolithic sites in danger? *Geomorphology* **2018**, *314*, 27–41. [CrossRef]
28. Ministry of Internal Affairs, Department for Emergency Situations and General Inspectorate for Emergency Situations. The Situation of the Accumulations under the Administration of D.A.Prut-S.G.A. from Iasi County, Annex No. 4. Available online: https://isujis.ro/wp-content/uploads/2016/04/anexa-4-SITUA%C5%A2IA-ACUMUL%C4%82RILOR.doc (accessed on 21 July 2021).
29. Climate Change—Department for Waters Forests and Fisheries National Administration "Romanian Waters" Management-Bucharest, National Institute of Hydrology and Water, Prut-Barlad River Basin Management Plan, 2016–2021, In Accordance with cu Article No. 2015. Available online: https://vdocuments.mx/plan-management-prut-barlad-31032015.html (accessed on 21 July 2021).
30. Arsene, C.; Olariu, R.I.; Mihalopoulos, N. Chemical composition of rainwater in the northeastern Romania, Iasi region (2003–2006). *Atmos. Environ.* **2007**, *41*, 9452–9467. [CrossRef]
31. Ward, J.H., Jr. Hierarchical grouping to optimize an objective function. *J. Am. Stat. Assoc.* **1963**, *58*, 236–244. [CrossRef]
32. Mathivanan, K.; Rajaram, R. Anthropogenic influences on toxic metals in water and sediment samples collected from industrially polluted Cuddalore coast, Southeast coast of India. *Environ. Earth Sci.* **2014**, *72*, 997–1010. [CrossRef]
33. Rahman, M.S.; Saha, N.; Molla, A.H.; Al-Reza, S.M. Assessment of Anthropogenic Influence on Heavy Metals Contamination in the Aquatic Ecosystem Components: Water, Sediment, and Fish. *Soil Sediment Contam.* **2014**, *23*, 353–373. [CrossRef]
34. Lin, Q.; Liu, E.; Zhang, E.; Li, K.; Shen, J. Spatial distribution, contamination and ecological risk assessment of heavy metals in surface sediments of Erhai Lake, a large eutrophic plateau lake in southwest China. *Catena* **2016**, *145*, 193–203. [CrossRef]
35. Li, X.; Yang, H.; Zhang, C.; Zeng, G.; Liu, Y.; Xu, W.; Wu, Y.; Lan, S. Spatial distribution and transport characteristics of heavy metals around an antimony mine area in central China. *Chemosphere* **2017**, *170*, 17–24. [CrossRef]
36. Kennedy, K.H. *Introduction to 3D Data Modeling whit ArcGIS 3D AnalystT and Google Earth*; John Wiley & Sons, Inc.: Hoboken, NJ, USA, 2009; ISBN 9780470548776.
37. Johnston, K.; Krivoruchko, K.; Lucas, N. *Using ArcGIS Geostatistical Analyst*; Esri: West Redlands, CA, USA, 2001.
38. Muranova, T.A.; Zinchenko, D.V.; Kononova, S.V.; Belova, N.A.; Miroshnikov, A.I. Plant protein hydrolysates as fish fry feed in aquaculture. Hydrolysis of rapeseed proteins by an enzyme complex from king crab hepatopancreas. *Appl. Biochem. Microbiol.* **2017**, *53*, 680–687. [CrossRef]

39. Quinto, B.P.T.; Albuquerque, J.V.; Bezerra, R.S.; Peixoto, S.; Soares, R. Replacement of fishmeal by two types of fish protein hydrolysate in feed for postlarval shrimp Litopenaeus vannamei. *Aquac. Nutr.* **2018**, *24*, 768–776. [CrossRef]
40. Daher, S.; Gülaçar, F. Geochemistry of carboxylic acids in the sediments from lake Cadagno (Switzerland). *Arch. Sci. C. R. Seances Soc.* **2005**, *58*, 25–42.
41. Jonsson, A.; Ström, L.; Åberg, J. Composition and variations in the occurrence of dissolved free simple organic compounds of an unproductive lake ecosystem in northern Sweden. *Biogeochemistry* **2007**, *82*, 153–163. [CrossRef]
42. Prychid, C.J.; Rudall, P.J. Calcium oxalate crystals in monocotyledons: A review of their structure and systematics. *Ann. Bot.* **1999**, *84*, 725–739. [CrossRef]
43. Smith, R.L.; Oremland, R.S. Anaerobic Oxalate Degradation: Widespread Natural Occurrence in Aquatic Sediments. *Appl. Environ. Microbiol.* **1983**, *46*, 106–113. [CrossRef] [PubMed]
44. Škrbić, B.; Durišić-Mladenović, N. Chemometric interpretation of heavy metal patterns in soils worldwide. *Chemosphere* **2010**, *80*, 1360–1369. [CrossRef] [PubMed]
45. Chapman, D. *Water Quality Assessments—A Guide to Use of Biota, Sediments and Water in Environmental Monitoring*, 2nd ed.; E&FN Spon: London, UK, 1996; ISBN 0419216006.
46. Cristini, P.A.; Tietze, E.; De Francesco, C.G.; Martínez, D.E. Water geochemistry of shallow lakes from the southeastern Pampa plain, Argentina and their implications on mollusk shells preservation. *Sci. Total Environ.* **2017**, *603–604*, 155–166. [CrossRef] [PubMed]
47. Acosta, J.A.; Jansen, B.; Kalbitz, K.; Faz, A.; Martínez-Martínez, S. Salinity increases mobility of heavy metals in soils. *Chemosphere* **2011**, *85*, 1318–1324. [CrossRef] [PubMed]
48. Roy, K.; Chari, M.S.; Gaur, S.R.; Thakur, A. Ecological dynamics and hydrobiological correlations in freshwater ponds-recent researches and application. *Int. J. Environ. Biol.* **2014**, *4*, 112–118. [CrossRef]
49. Dodds, W.K.; Jones, J.R.; Welch, E.B. Suggested classification of stream trophic state: Distributions of temperate stream types by chlorophyll, total nitrogen, and phosphorus. *Water Res.* **1998**, *32*, 1455–1462. [CrossRef]

atmosphere

MDPI

Article

Kinetic Measurements of Cl Atom Reactions with C_5–C_8 Unsaturated Alcohols

Asma Grira [1,2], Cornelia Amarandei [3], Manolis N. Romanias [1], Gisèle El Dib [2], André Canosa [2], Cecilia Arsene [3,4], Iustinian Gabriel Bejan [3,4], Romeo Iulian Olariu [3,4,*], Patrice Coddeville [1] and Alexandre Tomas [1,*]

1 IMT Lille Douai, Univ. Lille, SAGE—Sciences de l'Atmosphère et Génie de l'Environnement, 59000 Lille, France; asma.grira@univ-rennes1.fr (A.G.); emmanouil.romanias@imt-lille-douai.fr (M.N.R.); patrice.coddeville@imt-lille-douai.fr (P.C.)

2 CNRS, IPR (Institut de Physique de Rennes)-UMR 6251, Université de Rennes, F-35000 Rennes, France; gisele.eldib@univ-rennes1.fr (G.E.D.); andre.canosa@univ-rennes1.fr (A.C.)

3 Department of Chemistry, Faculty of Chemistry, 11 Carol I, "Alexandru Ioan Cuza" University of Iasi, 700506 Iasi, Romania; cornelia.amarandei@chem.uaic.ro (C.A.); carsene@uaic.ro (C.A.); iustinian.bejan@uaic.ro (I.G.B.)

4 Integrated Centre of Environmental Science Studies in the North Eastern Region, 11 Carol I, "Alexandru Ioan Cuza" University of Iasi, 700506 Iasi, Romania

* Correspondence: oromeo@uaic.ro (R.I.O.); alexandre.tomas@imt-lille-douai.fr (A.T.)

Received: 6 February 2020; Accepted: 29 February 2020; Published: 4 March 2020

Abstract: The reactions of five structurally similar unsaturated alcohols, i.e., (*Z*)-2-penten-1-ol, (*E*)-2-hexen-1-ol, (*E*)-3-hexen-1-ol, (*Z*)-3-hexen-1-ol, and 1-octen-3-ol, with Cl atoms in the gas phase, were investigated at 296 ± 2 K and 1 atm by the relative-rate kinetic technique using a 600-L Teflon reaction chamber. Selected ion flow tube mass spectrometry (SIFT-MS) was used simultaneously to monitor the decay of the alcohols of interest and selected reference compounds. Tetrahydrofuran (THF), propan-1-ol, and octane were used as reference compounds. Chlorine atoms were produced by the photolysis of molecular chlorine (Cl_2) using broadband actinic lamps near 365 nm. The estimated rate constant values (in 10^{-10} $cm^3 \cdot molecule^{-1} \cdot s^{-1}$) followed the order 2.99 ± 0.53 ((*Z*)-2-penten-1-ol) < 3.05 ± 0.59 ((*E*)-3-hexen-1-ol) < 3.15 ± 0.58 ((*Z*)-3-hexen-1-ol) < 3.41 ± 0.65 ((*E*)-2-hexen-1-ol) < 4.03 ± 0.77 (1-octen-3-ol). The present work provides the first value of the rate constant for the reaction of 1-octen-3-ol with Cl atoms. The results are discussed and interpreted in relation to other studies where literature data are available. The structure–activity relationship and the atmospheric implications are discussed as well.

Keywords: (*Z*)-2-penten-1-ol; (*E*)-2-hexen-1-ol; (*E*)-3-hexen-1-ol; (*Z*)-3-hexen-1-ol; 1-octen-3-ol; Cl atoms; kinetics; structure–activity relationship; SIFT-MS

1. Introduction

Volatile organic compounds (VOCs) are trace gases generally present in the troposphere at sub-ppb concentrations. Yet, they play a major role in the chemistry of the troposphere through the formation of free radicals, ozone, and potentially secondary organic aerosols (SOA) [1,2]. It is recognized that the amount of VOCs emitted from biogenic sources (BVOC) largely exceeds that released from anthropogenic sources (AVOC) [3,4]. Green leaf volatiles (GLV), such as unsaturated alcohols [5], are BVOCs which are emitted from vegetation either spontaneously or under stress conditions [6]. Moreover, their emissions may increase due to climate change [7]. Despite this, the atmospheric reactivity of these compounds is less studied with respect to other BVOCs like monoterpenes.

Several biological materials like grasses, grains, fruits, dried fruits, vegetables, trees, and shrubs were shown to be a source of (*Z*)-3-hexen-1-ol and a series of (*E*)-3-alken-1-ols in the atmosphere [8–10]. Unsaturated alcohols with longer carbon chains such as 1-octen-3-ol were detected in grass emissions such as clover [11,12] and fungi [13]. Some unsaturated alcohols such as (*Z*)-3-hexen-1-ol and 1-octen-3-ol released by wheat, oat, and barley grains are thought to be insect attractors [14]. Biotic and abiotic stress factors lead to plant damage and stimulate emissions of higher concentrations of unsaturated alcohols in the troposphere [8,15,16]. In the Austrian Alps, (*Z*)-2-penten-1-ol was detected at a few-ppb level and its presence in such an area was attributed to the peroxidation of fatty acids occurring as a result of freeze damage on leaves [17].

Once in the atmosphere, unsaturated alcohols can be removed via reactions with atmospheric oxidants such as OH and NO_3 radicals, O_3, and Cl atoms [18]. The average concentration of Cl atoms in the troposphere is on the order of 10^3–10^4 atoms·cm^{-3} but concentrations as high as 10^5 atoms·cm^{-3} were observed at dawn in the marine boundary layer. At such concentrations, the Cl-driven chemistry might play an important role in VOC oxidation in the troposphere [19–22]. In fact, as the OH concentration is on the order of 10^6 radicals·cm^{-3} [23], Cl could present a competitive oxidation process for various VOCs especially during morning hours, at the times of maximum rates of Cl-precursor photolysis [24,25]. Recent findings suggest that chlorine atom reactivity in the atmosphere could be important even far inward from the coasts [26,27], where $ClNO_2$ pools are highly available as important Cl atom reservoirs [28,29]. Moreover, for some specific sites, like landfills, the impact of chlorine atoms on the atmospheric oxidation capacity might bring up to 10 times higher contributions to the local processes [25]. The formation of chlorine atoms in the atmosphere proceeds mainly through the oxidation of HCl by OH radicals and the photolysis of photolabile chlorine reservoir compounds (Cl_2, $ClNO_2$, and BrCl) [28–30]. Heterogeneous reactions involving sea salt and ozone are also a source of Cl atoms in the marine boundary layer [31,32]. Over the last two decades, although several experimental and theoretical works debated the potential impact of Cl oxidation with numerous VOCs in the tropospheric chemistry [33–37], the reactivity of some unsaturated alcohols is still not well established.

The aim of the present study was to determine the rate constants for the reactions of the following series of unsaturated alcohols with Cl atoms:

$$(Z)\text{-2-penten-1-ol} + \text{Cl} \rightarrow \text{Products}, \quad (1)$$

$$(E)\text{-2-hexen-1-ol} + \text{Cl} \rightarrow \text{Products}, \quad (2)$$

$$(E)\text{-3-hexen-1-ol} + \text{Cl} \rightarrow \text{Products}, \quad (3)$$

$$(Z)\text{-3-hexen-1-ol} + \text{Cl} \rightarrow \text{Products}, \quad (4)$$

$$\text{1-octen-3-ol} + \text{Cl} \rightarrow \text{Products}. \quad (5)$$

The reactivity of these unsaturated alcohols with Cl atoms was scarcely investigated [18]. The kinetics of (*Z*)-2-penten-1-ol with Cl atoms was solely determined in 2010 in a 400-L Teflon bag, using off-line gas chromatography with a flame ionization detector (GC-FID) and following a relative-rate kinetic approach [38]. For unsaturated hexenols, the rate constants for (*E*)-2-hexen-1-ol, (*E*)-3-hexen-1-ol, and (*Z*)-3-hexen-1-ol were determined only once also using the relative-rate kinetic approach in a 1080-L quartz glass simulation chamber with in situ Fourier-transform infrared (FTIR) spectroscopy [39]. No data are available regarding the rate constant of 1-octen-3-ol with chlorine atoms. The present work represents the first study on the relative-rate constant kinetic approach for the 1-octen-3-ol and Cl reaction and the second for (*Z*)-2-penten-1-ol and the series of hexenols cited above. Moreover, it has to be emphasized that, to our knowledge, the present kinetic measurements were performed for the first time using a selected ion flow tube mass spectrometer (SIFT-MS). The SIFT-MS instrument was used to measure the time decay of the above-listed compounds. A consistent determination of

the reaction kinetics will help to better understand the atmospheric impacts of such compounds and develop structure–activity relationships for atmospheric chemistry models.

2. Experiments

Rate constants were measured at room temperature (296 ± 2 K) in zero air at atmospheric pressure (760 Torr) using the Thalamos simulation chamber which is a 600-L cubic Teflon photoreactor (Figure S1, Supplementary Materials). More details of the experimental set-up can be found elsewhere [40], and only a brief description is given hereafter. The Teflon bag of the chamber is fixed inside a temperature-controlled box which can be regulated between 231 and 453 K. The chamber is surrounded by a set of 20 ultraviolet (UV) lamps emitting around 365 nm (PL-L 24W/10/4P, Philips, The Netherlands). The lamps were used to produce Cl atoms through the photolysis of Cl_2. The chamber is equipped with inlet and outlet ports used for reactant injection and reaction mixture sampling, respectively. Two fans are mounted inside the reactor in order to ensure the homogeneity of the gas mixture.

In the present work initial concentrations of reactants were from 0.7 to 1.5 ppm for both alcohols and reference compounds and around 1.7 ppm for molecular chlorine. Such high organic concentrations are not expected to induce secondary chemistry, since reactions of organic peroxy radicals generated as intermediates in atmospheric chemical mechanisms react very slowly with organic compounds [41]. The reaction mixture was continuously pumped through a sample loop using a dry Teflon diaphragm pump and reinjected into the reaction chamber with a flow rate of 4 L·min^{-1}.

A Voice200® SIFT-MS (Syft Technologies, New Zealand) instrument connected to the loop sampled the chamber at 10 mL·min^{-1}, allowing the decays of the reactants (alcohols and reference compounds) to be recorded. The SIFT-MS used in this study contains technical features similar to those from its first design [42] and all additional descriptions can be found in other recent papers [43–46]. Details on the SIFT-MS efficiency in measuring unsaturated alcohols (including those investigated in the present study) and about the ion reaction mechanisms were reported by Schoon et al. [47]. The detection limit of the commercially available SIFT-MS is at about pptv levels with a time resolution of 1 s.

The SIFT-MS measurement process is started by the production of reagent ions (R^+: H_3O^+, NO^+, and O_2^+) in a microwave discharge of a mixture of zero air and water vapor. The reagent ions are focused on a first quadrupole mass filter. Every few milliseconds, a single ionic species is selected based on its mass-to-charge ratio (m/z). Then, the selected ion passes to the flow tube reactor in a stream of carrier gas (He at 1 Torr). In addition, the Thalamos gas sample enters into this flow tube and undergoes a soft ionization reaction depending on the chemical properties of its components (A) (either alcohol or reference compound in this work) such as proton affinity and ionization energies. The reaction between the reagent ions (R^+) and the components (A) generates ion products (P^+) and neutral products (N). These processes involve (i) ionization by H_3O^+ occurring mainly via proton transfer and water elimination, (ii) NO^+ reactions proceeding in different ways, such as charge transfer, hydride and/or hydroxide ion transfer, and/or three body association, and (iii) O_2^+ reactions generally occurring via charge transfer [43,47]. All these chemical species (R^+, A, P^+, and N) are injected into a second quadrupole mass filter in order to select ions based on their m/z. An electron multiplier detector placed at the exit of the second quadrupole is used to measure the count rates of the ions in the selected m/z range. In the present work, for SIFT-MS measurements, at least 10,000 counts were set as the limit before the instrument switched from one mass to another and the dwell time was on the order of one second. In addition, the mass spectrometer was internally calibrated on a daily basis with the help of a standard mixture of nine compounds provided by the supplier (Scotty, UN1956, Interscience, Belgium). The internal calibration procedure and the known reaction rate constants of the precursor ions with the analytes allow estimating the theoretical concentrations of any organic compound.

Table S1 (Supplementary Materials) summarizes all the product ions (P^+) observed for alcohols and references. To determine the relative rate constants, pairs of representative product ions from the used alcohol and reference compounds were selected and used to plot the reactant decays according to the relative-rate kinetic approach. The ions that could be used for the kinetic analysis were selected

based on the absence of any possible interference arising from other chemical processes happening simultaneously with the studied reaction. Therefore, a series of tests were carried out before any experiment, where only the compound of interest (either the alcohol or the reference) and Cl_2 were present and mixed with purified air in the Thalamos chamber. Gas samples were analyzed by SIFT-MS, selecting all the product ions arising from alcohols and references. The alcohol and reference product ions displaying interferences with reaction products ions were excluded from the analysis.

Each experiment started by cleaning the reaction chamber at least for 2 h at 50 °C using a flow rate of about 20 L·min^{-1} of zero air. Once the temperature of the reactor dropped to room temperature, the cleanliness of the reactor was evaluated by measuring the background levels of the selected ions for both alcohol and reference compound using the SIFT-MS system over 10 min. The background levels for all the selected ions never exceeded 5% of their initial experimental concentrations. Wall losses of the alcohols and the reference compounds in the dark were investigated in preliminary experiments, and negligible contributions were determined for these processes. The coefficient of variation (CV, expressed as the ratio of one standard deviation to the mean value of 40-min measurements) for the recorded signals showed <2.7% values. The reported values actually reflect small fluctuatios in the performances of the instrument such as small variations in the precursor ion concentrations, temperature of the instrument core, etc. The stability of the alcohols and reference compounds under UV-A irradiation was also tested, and all compounds were shown to be stable (CV < 2.8% over 30 min). The studied alcohol was injected in the chamber. The ion signal delivered by the SIFT-MS apparatus was recorded for 30 to 45 min until signal stabilization was achieved. The reference compound was then added to the reaction mixture and left to stabilize in the dark for 15 min. The precursor of chlorine atoms (Cl_2) was finally introduced into the reactor, and the mixture was left again for 20 min in the dark. The UV lamps were turned on for 30 min in order to monitor the reaction initiated by Cl atoms.

At the moment of Cl_2 injection in the dark, the alcohol concentration showed a very fast decay in its concentration in the first 2–3 min, which was immediately followed by stabilization. Alcohol decays were of the order of 5–10% for 1-octen-3-ol, 15–20% for (*Z*)-2-penten-1-ol, and about 30% for the C_6 alcohols. In the experimental set-up, the inlet and outlet ports are relatively close to each other (20 cm) and, therefore, it is believed that Cl_2 concentrations inside the injection port could be for a while up to 10^4 times higher than their final values in the chamber. These very high local concentrations of Cl_2 may accelerate the reaction with the studied alcohol in the dark within the first few minutes after Cl_2 injection. Details concerning such dark reactions were already reported in previous studies for similar structurally unsaturated compounds [38,39,48–50]. Nevertheless, these suspected side reactions are not expected to modify the kinetic measurements since (1) alcohol concentrations were stabilized a few minutes after the Cl_2 injection, and (2) studied kinetics between unsaturated alcohols and Cl atoms are very fast compared to the kinetics of these side reactions.

The relative-rate kinetic method was used to determine the *alcohol + Cl* rate constants. The alcohols of interest and reference compounds simultaneously react with *Cl* atoms with rate constants k_{Alc+Cl} and k_{Ref+Cl}, respectively.

$$Alcohol + Cl \xrightarrow{k_{Alc+Cl}} Products \quad (6)$$

$$Reference + Cl \xrightarrow{k_{Ref+Cl}} Products \quad (7)$$

Assuming that the alcohol and reference compounds only disappear through reaction with *Cl* atoms, their concentration changes between $t = 0$ and time t can be related through the following equation:

$$ln\frac{[Alc]_0}{[Alc]_t} = \frac{k_{Alc+Cl}}{k_{Ref+Cl}} \times ln\frac{[Ref]_0}{[Ref]_t}, \quad (8)$$

where $[Alc]_0$, $[Alc]_t$, $[Ref]_0$, and $[Ref]_t$ are the alcohol and reference concentrations at time 0 and t, respectively. Thus, a plot of $\ln([Alc]_0/[Alc]_t)$ vs. $\ln([Ref]_0/[Ref]_t)$ should yield a straight line whose

slope (b) is the rate constant ratio k_{Alc+Cl}/k_{Ref+Cl}. The uncertainty of the slope (σ) corresponds to the uncertainty of the fitting.

For each reference, using the determined slope (b) and the known k_{Ref+Cl}, the k_{Alc+Cl} values could be calculated. The uncertainty of the determined rate constant (Δk_{Alc+Cl}) was estimated with the following expression:

$$\Delta k_{Alc+Cl} = \sigma \times k_{Ref+Cl} + b \times \Delta k_{Ref+Cl}, \quad (9)$$

where σ and Δk_{Ref+Cl} are the uncertainties of the slope (b) and k_{Ref+Cl}, respectively. The final rate constant $k_{Average}$ and its uncertainty $\Delta k_{Average}$ (standard error of the mean) were calculated using Equations (10) and (11), respectively.

$$k_{Average} = \frac{\sum_{i=1}^{n} k_i}{n}, \quad (10)$$

$$\Delta k_{Average} = \sqrt{\frac{\sum_{i=1}^{n} (\Delta k_i)^2}{n}}, \quad (11)$$

where k_i and Δk_i represent k_{Alc+Cl} and Δk_{Alc+Cl} for each reference i, respectively.

Rate constant values for the Cl atom-initiated oxidation of the reference compounds used in the present work (i.e., tetrahydrofuran (THF), propan-1-ol, and octane) are well known and are (in 10^{-10} $cm^3 \cdot molecule^{-1} \cdot s^{-1}$) 2.39 ± 0.57 for *THF + Cl* [51–53], 1.60 ± 0.07 for *propan-1-ol + Cl* [54], and 3.91 ± 0.63 for *octane + Cl* [55–59]. Reported uncertainties on the rate constants of *THF + Cl* and *octane + Cl* (k_{THF+Cl} and $k_{octane+Cl}$) are 2σ, whereas no specification was mentioned for the uncertainty of $k_{propan\text{-}1\text{-}ol\ +Cl}$ ([54]).

The following chemicals were used as received: (*Z*)-2-penten-1-ol (≥96%, Aldrich, Saint-Quentin Fallavier, France), (*E*)-2-hexen-1-ol (≥95%, Aldrich, Saint-Quentin Fallavier, France), (*E*)-3-hexen-1-ol (97%, Aldrich, Saint-Quentin Fallavier, France), (*Z*)-3-hexen-1-ol (>98%, Fluka, Seelze, Germany), 1-octen-3-ol (≥ 98%, Aldrich, Saint-Quentin Fallavier, France), tetrahydrofuran (99.9%, Acros, Noisy-le-Grand, France), propan-1-ol (98.9%, Aldrich, Saint-Quentin Fallavier, France), and octane (>99%, Aldrich, Saint-Quentin Fallavier, France). Molecular chlorine (Cl_2) was from Air Products (10% ± 0.5% Cl_2 in 90% ± 0.2% N_2). Extra pure zero air was produced with a pure air generator (AZ-2020, Claind, Italy) with relative humidity (RH) <2 ppm, and CO and CO_2 < 80 ppb. N_2 was from Messer France (99.999%, RH < 3 ppm).

3. Results

3.1. Kinetic Measurements for (Z)-2-Penten-1-ol

Three experiments were performed for the (*Z*)-2-penten-1-ol reaction with Cl atoms in zero air. Each experiment was done with one of the three reference compounds (THF, propan-1-ol, and octane), with this strategy leading finally to three distinct determinations. The kinetic plots for (*Z*)-2-penten-1-ol using THF, propan-1-ol, and octane as reference compounds are displayed in Figure 1a–c, respectively, for all the selected combinations of fragment ions.

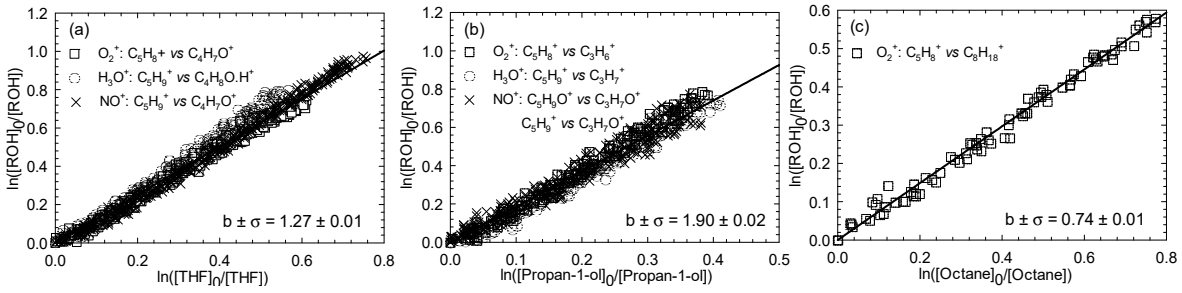

Figure 1. Relative loss of (*Z*)-2-penten-1-ol vs. that of tetrahydrofuran (THF) (**a**), propan-1-ol (**b**), and octane (**c**) in the Cl atom-initiated reaction.

The relative rate plots show very good linearity with zero intercepts, indicating absence of secondary reactions. Use of the known reference rate constants k_{Ref+Cl} allows k_{Alc+Cl} to be determined for each investigated situation. All the k_{Alc+Cl}/k_{Ref+Cl} ratios and the corresponding rate constant values for (*Z*)-2-penten-1-ol reactions with Cl atoms are reported in Table 1. For the (*Z*)-2-penten-1-ol with Cl atom reaction, an average rate constant value of (2.99 ± 0.53) × 10^{-10} $cm^3 \cdot molecule^{-1} \cdot s^{-1}$ was determined.

3.2. Kinetic Measurements for (*E*)-2-Hexen-1-ol, (*E*)-3-Hexen-1-ol, and (*Z*)-3-Hexen-1-ol

Kinetics of Cl atom with three hexenols, including (*E*)-2-hexen-1-ol, (*E*)-3-hexen-1-ol, and (*Z*)-3-hexen-1-ol, were investigated using the same reference compounds as in the case of (*Z*)-2-penten-1-ol. One experiment per reference was carried out. Figures 2–4 show the kinetic plots for the Cl reaction of (*E*)-2-hexen-1-ol (Figure 2), (*E*)-3-hexen-1-ol (Figure 3), and (*Z*)-3-hexen-1-ol (Figure 4), respectively.

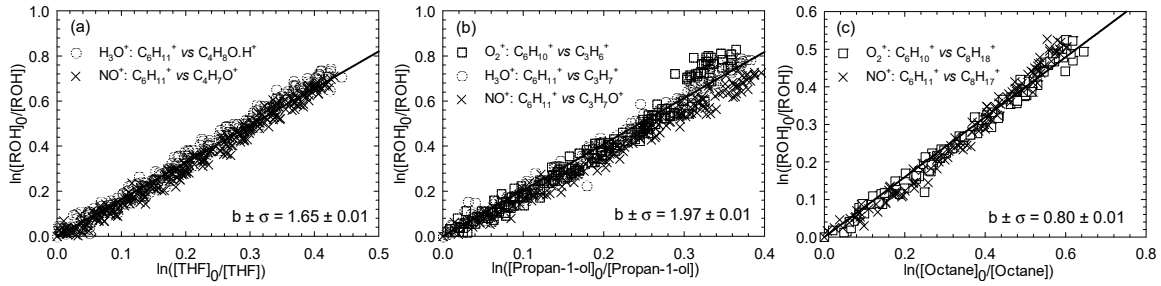

Figure 2. Relative loss of (*E*)-2-hexen-1-ol vs. that of THF (**a**), propan-1-ol (**b**), and octane (**c**) in the Cl atom-initiated reaction.

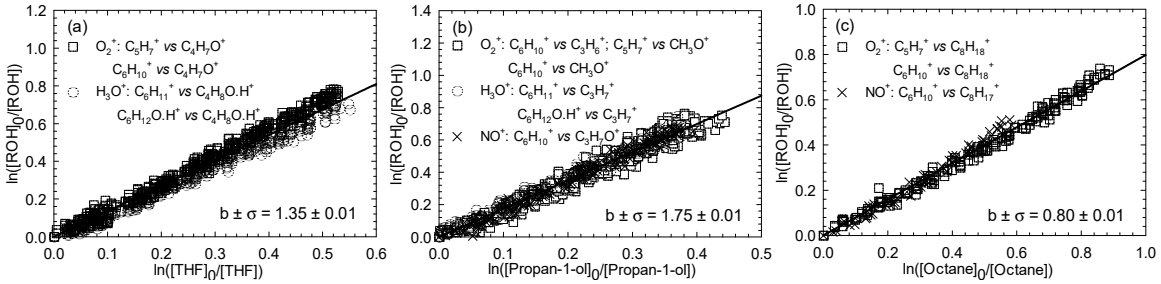

Figure 3. Relative loss of (*E*)-3-hexen-1-ol vs. that of THF (**a**), propan-1-ol (**b**), and octane (**c**) in the Cl atom-initiated reaction.

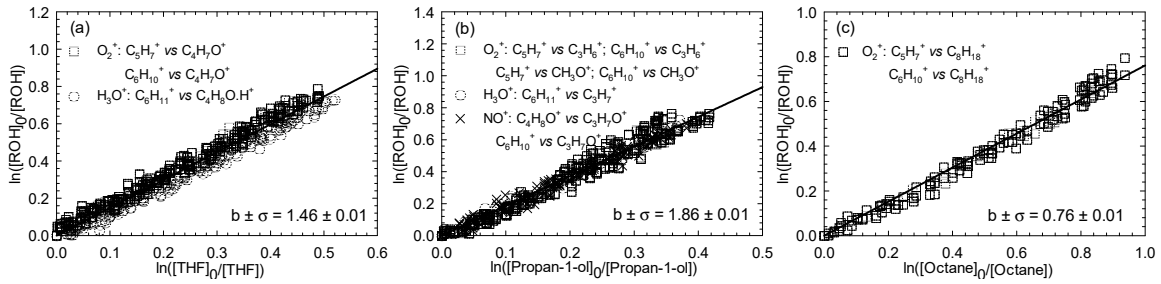

Figure 4. Relative loss of (*Z*)-3-hexen-1-ol vs. that of THF (**a**), propan-1-ol (**b**), and octane (**c**) in the Cl atom-initiated reaction.

A summary of the average rate constants determined for the reactions between Cl atoms and the three investigated unsaturated hexenols is given in Table 1. For the investigated alcohols reaction with Cl atoms, determined average rate constant values were 3.41 ± 0.65, 3.05 ± 0.59, and 3.15 ± 0.58 (× 10^{-10} $cm^3 \cdot molecule^{-1} \cdot s^{-1}$) for (*E*)-2-hexen-1-ol, (*E*)-3-hexen-1-ol, and (*Z*)-3-hexen-1-ol, respectively.

3.3. Kinetic Measurements for 1-Octen-3-ol

Six experiments were carried out for 1-octen-3-ol (two experiments for each reference compound used in the present study). Figure 5 displays the kinetic plots corresponding to the performed experiments.

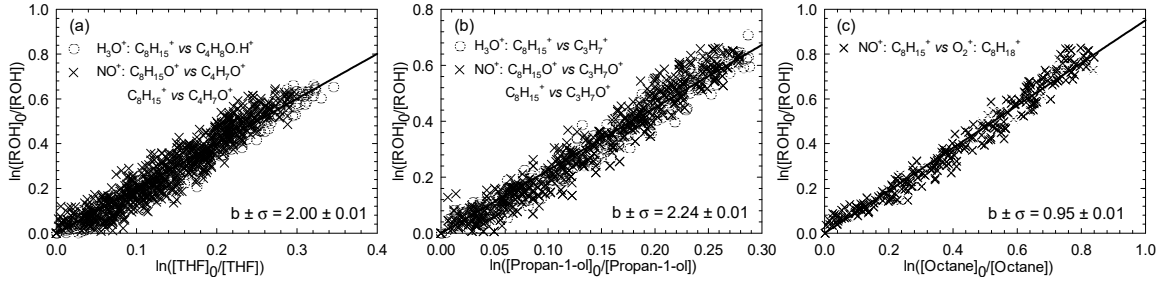

Figure 5. Relative loss of 1-octen-3-ol vs. that of THF (**a**), propan-1-ol (**b**), and octane (**c**) in the Cl atom-initiated reaction.

All the k_{Alc+Cl}/k_{Ref+Cl} ratios and the corresponding rate constants for each reference compound are reported in Table 1. The average rate constant for the Cl atom reaction with 1-octen-3-ol at 296 K was $(4.03 \pm 0.77) \times 10^{-10}$ cm^3·molecule^{-1}·s^{-1}.

4. Discussion

4.1. Summary of All the Determined Rate Constants and Comparison with Literature Data

The obtained rate constants (in 10^{-10} cm^3·molecule^{-1}·s^{-1}) are summarized in Table 1 and compared with the available literature data. All the details for the calculations were explained above in the experimental description.

Table 1. Summary of all the rate constants for the reactions of alcohols with Cl atoms (all rate constants are expressed in 10^{-10} cm^3·molecule^{-1}·s^{-1}).

Compound	Reference Compound						Average $k_{Average}$	Literature
	THF		Propan-1-ol		Octane			
	$\frac{k_{Alc+Cl}}{k_{Ref+Cl}}$	k_{Alc+Cl}	$\frac{k_{Alc+Cl}}{k_{Ref+Cl}}$	k_{Alc+Cl}	$\frac{k_{Alc+Cl}}{k_{Ref+Cl}}$	k_{Alc+Cl}		
(*Z*)-2-Penten-1-ol	1.27 ± 0.01	3.04 ± 0.75	1.90 ± 0.02	3.04 ± 0.17	0.74 ± 0.01	2.89 ± 0.51	2.99 ± 0.53	3.00 ± 0.49 [38]
(*E*)-2-Hexen-1-ol	1.65 ± 0.01	3.94 ± 0.96	1.97 ± 0.01	3.15 ± 0.15	0.80 ± 0.01	3.13 ± 0.54	3.41 ± 0.65	3.49 ± 0.82 [39]
(*E*)-3-Hexen-1-ol	1.35 ± 0.01	3.23 ± 0.79	1.75 ± 0.01	2.80 ± 0.14	0.80 ± 0.01	3.13 ± 0.62	3.05 ± 0.59	3.42 ± 0.79 [39]
(*Z*)-3-Hexen-1-ol	1.46 ± 0.01	3.49 ± 0.86	1.86 ± 0.01	2.98 ± 0.15	0.76 ± 0.01	2.97 ± 0.52	3.15 ± 0.58	2.94 ± 0.72 [39]
1-Octen-3-ol	2.00 ± 0.01	4.78 ± 1.16	2.24 ± 0.01	3.58 ± 0.17	0.95 ± 0.01	3.71 ± 0.64	4.03 ± 0.77	(*)

Note: (*) no data.

For the (*Z*)-2-penten-1-ol and Cl atom reaction, Rodríguez et al. [38] reported a rate constant value determined by the relative-rate kinetic method with CCl_3COCl as the Cl atom precursor. In this study octane, propene, and cyclohexane were used as reference compounds. The average value between the three determinations of Rodríguez et al. [38] was 3.00×10^{-10} cm^3·molecule^{-1}·s^{-1}. This value is in excellent agreement with the value determined in the present study (2.99×10^{-10} cm^3·molecule^{-1}·s^{-1}).

A series of reactions between Cl atoms and several unsaturated alcohols was investigated by Gibilisco et al. [39] using Cl_2 as a source of Cl atoms. Three hexenols among this series were also studied in the present work. The obtained rate constants are in good agreement with Gibilisco et al. [39], with the relative differences between our determinations and Gibilisco et al.'s determinations [39]

being of the order of 10% or less for all hexenols. For 1-octen-3-ol, no other measurements are available in the literature.

Although, for 1-octen-3-ol, the rate constant values determined with THF as reference compound appear to be higher than those determined using propan-1-ol and octane, the values are reported as obtained since (i) these systematic higher values were not observed for C_5 alkenols, and (ii) if necessary, the rate coefficient values for the alkenol reaction with Cl atom can be easily calculated by averaging the values obtained with the other two reference compounds. Moreover, one should also note that similar differences were observed for the hexenols. This may indicate a systematic error on $k(THF + Cl)$ and, therefore, further studies on $k(THF + Cl)$ are needed.

4.2. Structure–Activity Relationships

The reactions between unsaturated VOCs and Cl atoms proceed mainly via the addition to the double bond to produce a chlorine-containing alkyl radical. Addition occurs preferably on the least substituted carbon, thus forming the most stable radical [60]. This chlorinated alkyl radical adds O_2 to form a chlorinated peroxy radical whose further reactions lead to oxygenated chlorine-containing compounds [48]. A second minor pathway is the abstraction of the allylic hydrogen from the C–H bond. For example, a very recent work showed that the reaction of (*Z*)-3-hexene proceeds via both Cl atom addition and hydrogen abstraction with branching ratios of around 70% and 30%, respectively [61].

4.2.1. Effect of the Chain Length

Table S2 (Supplementary Materials) presents a synthesis of all the known rate constants of unsaturated *alcohol* + *Cl* from C_3 to C_8. The comparison of these data could help to better understand the relationships between molecular structure and rate constants. For a group of alcohols with the alcohol function located on the first carbon atom (alken-1-ol) and a C=C bond placed the second or third carbon atom, data are presented in Figure 6 for comparison purposes.

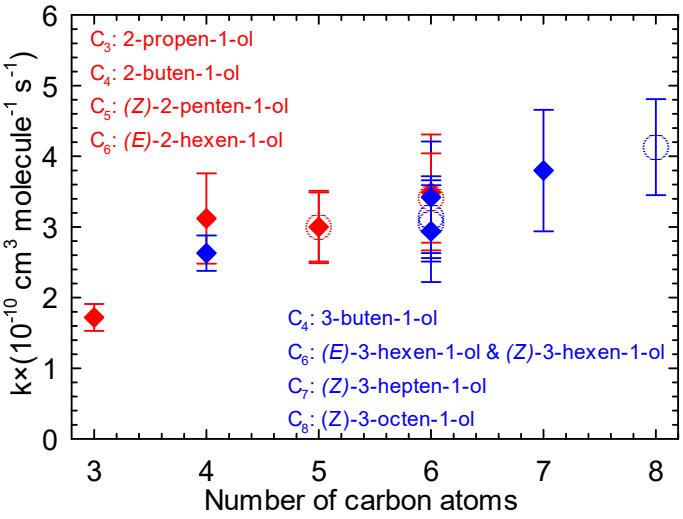

Figure 6. Rate constants of the reaction of Cl atoms with 2-alken-1-ols (red) and 3-alken-1-ols (blue) vs. number of carbon atoms (the open circles represent the values of the current study).

Considering the series of 2-alken-1-ols (red) with 2-propen-1-ol [49], 2-buten-1-ol [50], (*Z*)-2-penten-1-ol ([38] and this work), and (*E*)-2-hexen-1-ol ([39] and this work), the increase in chain length seems to lead to higher rate constants. A similar trend is also observable for the reaction of Cl atoms with the series of 3-alken-1-ols (blue) with 3-buten-1-ol [62], (*E*)-3-hexen-1-ol, (*Z*)-3-hexen-1-ol ([39] and this work), (*Z*)-3-hepten-1-ol, and (*Z*)-3-octen-1-ol [39]. The activation effect of the chain length on the rate constants was also observed in previous works for the reaction of Cl atoms with linear alcohols [63] and alkenes [22,64–66].

4.2.2. Effect of the OH Group

In order to better understand the role of the OH group in the unsaturated alcohol chains, the rate constants for the reaction of five unsaturated alcohols with Cl atoms were compared to the rate constants of their corresponding alkenes reaction with Cl atoms (Figure 7).

Table S3 (Supplementary Materials) lists the rate constants for the reactions of Cl atoms with a series of alkenes, i.e., propene, 1-butene, 1-pentene, *cis*-3-hexene, and 1-octene. Comparing the data presented in Tables S2 and S3 (Supplementary Materials) clearly shows that the rate constants for the reactions of Cl atoms with propene [67], 1-butene [65], 1-pentene [22], and 1-octene [66] are higher than the rate constants for the reactions of Cl atoms with 2-propen-1-ol [49], 3-buten-1-ol [62], 1-penten-3-ol [38], and 1-octen-3-ol (this work), respectively. A similar trend is observed when comparing (*Z*)-3-hexene + Cl [61] and (*Z*)-3-hexen-1-ol + Cl ([39] and this work). However, the data from the present work prove also that the presence of the hydroxyl group in the molecular structure clearly has a deactivating effect on the kinetics of unsaturated alcohols with Cl atoms through a negative inductive influence.

Moreover, Gibilisco et al. [39] suggested a stronger deactivating effect of the OH group for α-alkenols compared to β-alkenols based on literature data. Yet, the present results do not confirm this assumption, probably because the measured rate constants are close to the collision rate. Finally, it can be underlined that an activating effect of the OH group was observed for OH radical addition to alkenols [68], suggesting different reaction mechanisms.

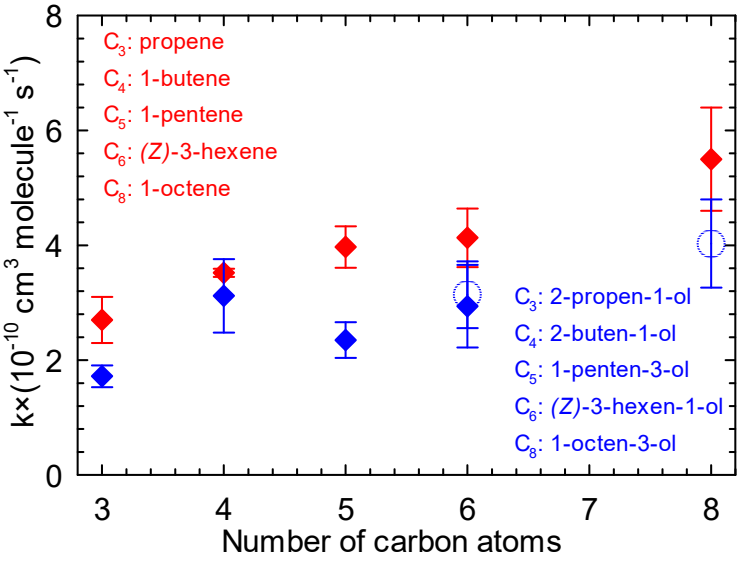

Figure 7. Rate constant of the reaction of Cl atoms with a series of alkenes (red) and alken-1-ols (blue) vs. number of carbon atoms (the open circles represent the values of the current study).

4.3. Atmospheric Implications

Atmospheric lifetimes τ_X of the studied alkenols were calculated using the expression $\tau_X = 1/k_X[X]$, with k_X being the rate constant for alkenol reaction with the oxidant X (Cl, OH, NO_3, or O_3) with an average concentration $[X]$. For the unsaturated alcohols investigated in the present work, the atmospheric lifetime with respect to Cl atom-induced reactions was estimated considering rate constant values expressed as averages of those determined in this work and in previous works. The following typical oxidant atmospheric concentrations were considered: (i) for Cl atoms, $[Cl] = 1 \times 10^4$ molecule·cm^{-3} [69] as representative of continental background atmosphere, and $[Cl] = 1 \times 10^5$ molecule·cm^{-3} as representative of the marine boundary layer and coastal areas [20,22,70], (ii) for O_3, $[O_3] = 7 \times 10^{11}$ molecule·cm^{-3} [71], (iii) for NO_3, a 12-h nighttime average NO_3 concentration of 5×10^8 molecule−cm^{-3} [72], and (iv) for OH, a 12-h daylight average OH concentration of 2×10^6 molecule·cm^{-3} [73]. Estimated atmospheric lifetimes are displayed in Table 2.

Table 2. Calculated atmospheric lifetimes for the reactions of the studied unsaturated alcohols with Cl, O_3, NO_3, and OH. Cl-low and Cl-high refer to [Cl] of 1×10^4 and 1×10^5 atoms·cm^{-3}, respectively.

Alkenol	τ_{Cl}(h) Cl-Low	τ_{Cl}(h) Cl-High	τ_{O_3}(h)	τ_{NO_3}(h)	τ_{OH}(h)
(*Z*)-2-Penten-1-ol	93 [(a)]	9.3 [(a)]	2.35 [(b)]	3.56 [(b)]	1.31 [(b)]
(*E*)-2-Hexen-1-ol	81 [(c)]	8.1 [(c)]	(*)	4.27 [(d)]	1.39 [(e)]
(*E*)-3-Hexen-1-ol	86 [(c)]	8.6 [(c)]	(*)	1.25 [(d)]	1.32 [(f)]
(*Z*)-3-Hexen-1-ol	91 [(c)]	9.1 [(c)]	4.70 [(b)]	2.06 [(g)]	1.24 [(h)]
1-Octen-3-ol	69 [(i)]	6.9 [(i)]	(*)	(*)	(*)

Note: [(a)] ([38], this work); [(b)] [18]; [(c)] ([39], this work); [(d)] [74]; [(e)] [75]; [(f)] [75–77]; [(g)] [74,78]; [(h)] [75,78–80]; [(i)] this work; [(*)] no data.

The estimated atmospheric lifetimes of the studied alcohols for their reactions with the atmospheric oxidants range from 1.24 to 4.7 h, except for the reactions with Cl atoms for which much higher lifetimes were found in a continental background atmosphere. Thus, C_5–C_8 unsaturated alcohols are rapidly removed in the gas phase by O_3, NO_3, or OH and disappear closely to their emission sources. Yet, it is worth stressing that, in the marine boundary layer and in coastal areas, the Cl-initiated oxidation of alkenols can become competitive compared to other oxidants with lifetimes on the order of a few hours. In addition to the marine boundary layer and coastal areas, specific continental areas were recently shown to display even higher Cl atom concentrations [27,81,82]. The present results will help in better understanding the atmospheric chemistry in these regions.

5. Conclusions

In the present work, five structurally similar unsaturated alcohols including (*Z*)-2-penten-1-ol, (*E*)-2-hexen-1-ol, (*E*)-3-hexen-1-ol, (*Z*)-3-hexen-1-ol, and 1-octen-3-ol were investigated with regard to their reactivity toward Cl atoms. Investigations were performed in a 600-L Teflon reaction chamber at 296 ± 2 K and 1 atm zero air. The relative-rate kinetic approach was used to determine rate constant values of the target unsaturated alcohols reaction with Cl atoms produced by the photolysis of molecular chlorine. Tetrahydrofuran, propan-1-ol, and octane were used as reference compounds. For the first time, the decays of alkenols and reference compounds were monitored using selected ion flow tube mass spectrometry (SIFT-MS).

The rate constant values (in 10^{-10} cm^3·molecule^{-1}·s^{-1}) determined in the present work, 2.99 ± 0.53 for (*Z*)-2-penten-1-ol, 3.05 ± 0.59 for (*E*)-3-hexen-1-ol, 3.15 ± 0.58 for (*Z*)-3-hexen-1-ol, 3.41 ± 0.65 for (*E*)-2-hexen-1-ol, and 4.03 ± 0.77 for 1-octen-3-ol, within the experimental error limits, are in very good agreement with literature data. The present work reports, for the first time, the rate constant value for the reaction between 1-octen-3-ol and Cl atoms. Data obtained in the present work proves the activation effect of the chain length on the rate constants values specific for the kinetics between alkenols and Cl atoms. Moreover, evidence was obtained of the effect of the hydroxyl group presence in the molecular structure, with a deactivating effect on the kinetics of unsaturated alcohols with Cl atoms through negative inductive influence. The atmospheric lifetimes estimated in the present work with regard to atmospheric oxidant abundances suggest that alkenol reactivity toward Cl atoms becomes an important competitive process in alkenol sinks, especially in marine boundary layer and coastal areas.

Supplementary Materials: The following are available online at http://www.mdpi.com/2073-4433/11/3/256/s1. Figure S1: General description of Thalamos facility, Table S1: Product ion distributions of the H_3O^+, NO^+, and O_2^+ reactions with the studied unsaturated alcohols and reference compounds (BR—branching ratios of product ions; data come from the SIFT-MS library; BR could vary depending on the experimental conditions and working status of the instrument), Table S2: Rate constants for the reactions of Cl atoms with unsaturated alcohols at 298 K and atmospheric pressure (all rate constants are expressed in 10^{-10} cm^3·molecule^{-1}·s^{-1}), Table S3: Rate constants for the reactions of Cl atoms with alkenes at 298 K and atmospheric pressure (all rate constants are expressed in 10^{-10} cm^3·molecule^{-1}·s^{-1}).

Author Contributions: Data curation, A.G., C.A. (Cornelia Amarandei) and M.N.R.; Formal analysis, A.G., M.N.R., C.A. (Cecilia Arsene), I.G.B., R.I.O. and A.T.; Funding acquisition, C.A. (Cornelia Amarandei), R.I.O. and A.T.; Investigation, A.G. and C.A. (Cornelia Amarandei); Methodology, A.G., M.N.R., R.I.O. and A.T.; Project administration, G.E.D., A.C., R.I.O., P.C. and A.T.; Resources, R.I.O. and A.T.; Supervision, G.E.D., A.C., C.A. (Cecilia Arsene), I.G.B., R.I.O. and A.T.; Validation, M.N.R., C.A. (Cecilia Arsene), I.G.B., R.I.O. and A.T.; Visualization, A.G., C.A. (Cornelia Amarandei), M.N.R., C.A. (Cecilia Arsene), I.G.B., R.I.O. and A.T.; Writing—original draft, A.G., C.A. (Cecilia Arsene) and R.I.O.; Writing—review & editing, M.N.R., G.E.D., A.C., C.A. (Cecilia Arsene), R.I.O., P.C. and A.T. All authors have read and agreed to the published version of the manuscript.

Funding: SAGE laboratory acknowledges funding by the French ANR agency under contract No. ANR-11-LabX-0005-01 CaPPA (Chemical and Physical Properties of the Atmosphere), the Région Hauts-de-France, the Ministère de l'Enseignement Supérieur et de la Recherche (CPER Climibio), and the European Fund for Regional Economic Development. A.G. is grateful for a PhD grant from Brittany Region and IMT Lille Douai. Authors from French laboratories are grateful to the INSU-LEFE-CHAT program for funding this research. All the authors are thankful to the PHC Brancusi program for funding the OzOA project (38385UD). C.A., I.G.B., R.I.O., and A.T. acknowledge the financial support from European Union's Horizon 2020 Research and Innovation Framework Program, through the EUROCHAMP-2020 Infrastructure Activity Grant (grant agreement No 730997).

Conflicts of Interest: The authors declare no conflicts of interest.

References

1. Atkinson, R.; Arey, J. Gas-phase tropospheric chemistry of biogenic volatile organic compounds: A review. *Atmos. Environ.* **2003**, *37*, 197–219. [CrossRef]
2. Hallquist, M.; Wenger, J.C.; Baltensperger, U.; Rudich, Y.; Simpson, D.; Claeys, M.; Dommen, J.; Donahue, N.M.; George, C.; Goldstein, A.H.; et al. The formation, properties and impact of secondary organic aerosol: Current and emerging issues. *Atmos. Chem. Phys.* **2009**, *9*, 5155–5236. [CrossRef]
3. Guenther, A.; Hewitt, C.N.; Erickson, D.; Fall, R.; Geron, C.; Graedel, T.; Harley, P.; Klinger, L.; Lerdau, M.; McKay, W.A.; et al. A global model of natural volatile organic compound emissions. *J. Geophys. Res. Atmos.* **1995**, *100*, 8873–8892. [CrossRef]
4. Peñuelas, J.; Staudt, M. BVOCs and global change. *Trends Plant Sci.* **2010**, *15*, 133–144. [CrossRef] [PubMed]
5. König, G.; Brunda, M.; Puxbaum, H.; Hewitt, C.N.; Duckham, S.C.; Rudolph, J. Relative contribution of oxygenated hydrocarbons to the total biogenic VOC emissions of selected mid-European agricultural and natural plant species. *Atmos. Environ.* **1995**, *29*, 861–874.
6. Loreto, F.; Schnitzler, J.P. Abiotic stresses and induced BVOCs. *Trends Plant Sci.* **2010**, *15*, 154–166. [CrossRef]
7. Kleist, E.; Mentel, T.F.; Andres, S.; Bohne, A.; Folkers, A.; Kindler-Scharr, A.; Rudich, Y.; Springer, M.; Tillmann, R.; Wildt, J. Irreversible impacts of heat on the emissions of monoterpenes, sesquiterpenes, phenolic BVOC and green leaf volatiles from several tree species. *Biogeosciences* **2012**, *9*, 5111–5123. [CrossRef]
8. Arey, J.; Winer, A.M.; Atkinson, R.; Aschmann, S.M.; Long, W.D.; Morrison, C.L. The emission of (Z)-3-hexen-1-ol, (Z)-3-hexenylacetate and other oxygenated hydrocarbons from agricultural plant species. *Atmos. Environ. Part A Gen. Top.* **1991**, *25*, 1063–1075. [CrossRef]
9. Yilmaz, E. The chemistry of fresh tomato flavor. *Turk. J. Agric. For.* **2001**, *25*, 149–155.
10. Lorber, K.; Buettner, A. Structure–odor relationships of (E)-3-alkenoic acids, (E)-3-alken-1-ols, and (E)-3-alkenals. *J. Agric. Food Chem.* **2015**, *63*, 6681–6688. [CrossRef]
11. Buttery, R.G.; Kamm, J.A. Volatile components of alfalfa: Possible insect host plant attractants. *J. Agric. Food Chem.* **1980**, *28*, 978–981. [CrossRef]
12. Kline, D.L.; Allan, S.A.; Bernier, U.R.; Welch, C.H. Evaluation of the enantiomers of 1-octen-3-ol and 1-octyn-3-ol as attractants for mosquitoes associated with a freshwater swamp in Florida, USA. *Med. Vet. Entomol.* **2007**, *21*, 323–331. [CrossRef] [PubMed]
13. Kaminski, E.; Stawicki, S.; Wasowicz, E. Volatile flavor compounds produced by molds of Aspergillus, *Penicillium*, and *Fungi* imperfecti. *Appl. Environ. Microbiol.* **1974**, *27*, 1001–1004. [CrossRef]
14. Buttery, R.G.; Ling, L.C.; Wellso, S.G. Oat leaf volatiles: Possible insect attractants. *J. Agric. Food Chem.* **1982**, *30*, 791–792. [CrossRef]
15. Croft, K.P.; Juttner, F.; Slusarenko, A.J. Volatile products of the lipoxygenase pathway evolved from Phaseolus vulgaris (L.) leaves inoculated with Pseudomonas syringae pv phaseolicola. *Plant Physiol.* **1993**, *101*, 13–24. [CrossRef] [PubMed]

16. Heiden, A.C.; Kobel, K.; Langebartels, C.; Schuh-Thomas, G.; Wildt, J. Emissions of oxygenated volatile organic compounds from plants Part I: Emissions from lipoxygenase activity. *J. Atmos. Chem.* **2003**, *45*, 143–172. [CrossRef]
17. Karl, T.; Fall, R.; Crutzen, P.J.; Jordan, A.; Lindinger, W. High concentrations of reactive biogenic VOCs at a high altitude site in late autumn. *Geophys. Res. Lett.* **2001**, *28*, 507–510. [CrossRef]
18. Calvert, J.; Mellouki, A.; Orlando, J. *Mechanisms of Atmospheric Oxidation of the Oxygenates*; Oxford University Press: New York, NY, USA, 2011.
19. Pszenny, A.A.P.; Keene, W.C.; Jacob, D.J.; Fan, S.; Maben, J.R.; Zetwo, M.P.; Springer-Young, M.; Galloway, J.N. Evidence of inorganic chlorine gases other than hydrogen chloride in marine surface air. *Geophys. Res. Lett.* **1993**, *20*, 699–702. [CrossRef]
20. Spicer, C.W.; Chapman, E.G.; Finlayson-Pitts, B.J.; Plastridge, R.A.; Hubbe, J.M.; Fast, J.D.; Berkowitz, C.M. Unexpectedly high concentrations of molecular chlorine in coastal air. *Nature* **1998**, *394*, 353. [CrossRef]
21. Tackett, P.J.; Cavender, A.E.; Keil, A.D.; Shepson, P.B.; Bottenheim, J.W.; Morin, S.; Deary, J.; Steffen, A.; Doerge, C. A study of the vertical scale of halogen chemistry in the Arctic troposphere during Polar Sunrise at Barrow, Alaska. *J. Geophys. Res. Atmos.* **2007**, *112*, 7. [CrossRef]
22. Ezell, M.J.; Wang, W.; Ezell, A.A.; Soskin, G.; Finlayson-Pitts, B.J. Kinetics of reactions of chlorine atoms with a series of alkenes at 1 atm and 298 K: Structure and reactivity. *Phys. Chem. Chem. Phys.* **2002**, *4*, 5813–5820. [CrossRef]
23. Lawrence, M.G.; Jöckel, P.; Kuhlmann, R.V. What does the global mean OH concentration tell us? *Atmos. Chem. Phys.* **2001**, *1*, 37–49. [CrossRef]
24. Tanaka, P.L.; Riemer, D.D.; Chang, S.; Yarwood, G.; McDonald-Butler, E.C.; Apel, E.C.; Orlando, J.J.; Silva, P.J.; Jimenez, J.L.; Canagaratna, M.R.; et al. Direct evidence for chlorine-enhanced urban ozone formation in Houston, Texas. *Atmos. Environ.* **2003**, *37*, 1393–1400. [CrossRef]
25. Bannan, T.J.; Anwar, M.; Khan, H.; Le Breton, M.; Priestley, M.; Worrall, S.D.; Bacak, A.; Marsden, N.A.; Lowe, D.; Pitt, J.; et al. A large source of atomic chlorine from $ClNO_2$ photolysis at a U.K. landfill site. *Geophys. Res. Lett.* **2019**, *46*, 8508–8516. [CrossRef]
26. Young, C.J.; Washenfelder, R.A.; Edwards, P.M.; Parrish, D.D.; Gilman, J.B.; Kuster, W.C.; Mielke, L.H.; Osthoff, H.D.; Tsai, C.; Pikelnaya, O.; et al. Chlorine as a primary radical: Evaluation of methods to understand its role in initiation of oxidative cycles. *Atmos. Chem. Phys.* **2014**, *14*, 3427–3440. [CrossRef]
27. Lee, B.H.; Lopez-Hilfiker, F.D.; Schroder, J.C.; Campuzano-Jost, P.; Jimenez, J.L.; McDuffie, E.E.; Fibiger, D.L.; Veres, P.R.; Brown, S.S.; Campos, T.L.; et al. Airborne observations of reactive inorganic chlorine and bromine species in the exhaust of coal-fired power plants. *J. Geophys. Res. Atmos.* **2018**, *123*, 11–225. [CrossRef] [PubMed]
28. Osthoff, H.D.; Roberts, J.M.; Ravishankara, A.R.; Williams, E.J.; Lerner, B.M.; Sommariva, R.; Bates, T.S.; Coffman, D.; Quinn, P.K.; Dibb, J.E.; et al. High levels of nitryl chloride in the polluted subtropical marine boundary layer. *Nat. Geosci.* **2008**, *1*, 324–328. [CrossRef]
29. Thornton, J.A.; Kercher, J.P.; Riedel, T.P.; Wagner, N.L.; Cozic, J.; Holloway, J.S.; Dubé, W.P.; Wolfe, G.M.; Quinn, P.K.; Middlebrook, A.M.; et al. A large atomic chlorine source inferred from mid-continental reactive nitrogen chemistry. *Nature* **2010**, *464*, 271–274. [CrossRef]
30. Crisp, T.A.; Lerner, B.M.; Williams, E.J.; Quinn, P.K.; Bates, T.S.; Bertram, T.H. Observations of gas phase hydrochloric acid in the polluted marine boundary layer. *J. Geophys. Res. Atmos.* **2014**, *119*, 6897–6915. [CrossRef]
31. Oum, K.W.; Lakin, M.J.; DeHaan, D.O.; Brauers, T.; Finlayson-Pitts, B.J. Formation of molecular chlorine from the photolysis of ozone and aqueous sea-salt particles. *Science* **1998**, *279*, 74–76. [CrossRef]
32. Vogt, R.; Crutzen, P.J.; Sander, R. A mechanism for halogen release from sea-salt aerosol in the remote marine boundary layer. *Nature* **1996**, *383*, 327–330. [CrossRef]
33. Knipping, E.M.; Dabdub, D. Impact of chlorine emissions from sea-salt aerosol on coastal urban ozone. *Environ. Technol.* **2003**, *37*, 275–284. [CrossRef] [PubMed]
34. Sahu, L.K. Reactive halogens and their measurements in the troposphere. *Indian J. Geo Mar. Sci.* **2014**, *43*, 1615–1622.

35. Barrera, J.A.; Garavagno, M.D.L.A.; Dalmasso, P.R.; Taccone, R.A. Atmospheric chemistry of 3-methoxy-1-propanol and 3-methoxy-1-butanol: Kinetics with OH radicals and Cl atoms, identification of the end-products in the presence of NO, mechanisms and atmospheric implications. *Atmos. Environ.* **2019**, *202*, 28–40. [CrossRef]
36. Tajuelo, M.; Bravo, I.; Rodríguez, A.; Aranda, A.; Díaz-de-Mera, Y.; Rodríguez, D. Atmospheric sink of styrene, α-methylstyrene, trans-β-methylstyrene and indene: Rate constants and mechanisms of Cl atom-initiated degradation. *Atmos. Environ.* **2019**, *200*, 78–89. [CrossRef]
37. Dhulipala, S.V.; Bhandari, S.; Ruiz, L.H. Formation of oxidized organic compounds from Cl-initiated oxidation of toluene. *Atmos. Environ.* **2019**, *199*, 265–273. [CrossRef]
38. Rodríguez, A.; Rodríguez, D.; Garzón, A.; Soto, A.; Aranda, A.; Notario, A. Kinetics and mechanism of the atmospheric reactions of atomic chlorine with 1-penten-3-ol and (Z)-2-penten-1-ol: An experimental and theoretical study. *Phys. Chem. Chem. Phys.* **2010**, *12*, 12245–12258.
39. Gibilisco, R.G.; Bejan, I.; Barnes, I.; Wiesen, P.; Teruel, M.A. Rate coefficients at 298 K and 1 atm for the tropospheric degradation of a series of C_6, C_7 and C_8 biogenic unsaturated alcohols initiated by Cl atoms. *Atmos. Environ.* **2014**, *94*, 564–572. [CrossRef]
40. Osseiran, N.; Romanias, M.N.; Gaudion, V.; Angelaki, M.; Papadimitriou, V.C.; Tomas, A.; Coddeville, P.; Thevenet, F. Development and validation of a THermALly regulated AtMOSpheric simulation chamber (THALAMOS). A versatile tool to simulate atmospheric processes. *J. Environ. Sci.* **2020**. (accepted).
41. Selby, K.; Waddington, D.J. Reactions of oxygenated radicals in the gas phase. Part 5. Reactions of methylperoxyl radicals and alkenes. *J. Chem. Soc. Perkin Trans. II* **1980**, 65–67. [CrossRef]
42. Adams, N.G.; Smith, D. The selected ion flow tube (SIFT); a technique for studying ion-neutral reactions. *Int. J. Mass Spectrom. Ion. Phys.* **1976**, *21*, 349–359. [CrossRef]
43. Španěl, P.; Smith, D. Selected ion flow tube studies of the reactions of H_3O^+, NO^+, and $O_2{}^+$ with several aromatic and aliphatic hydrocarbons. *Int. J. Mass Spectrom.* **1998**, *181*, 1–10. [CrossRef]
44. Diskin, A.M.; Wang, T.; Smith, D.; Španěl, P. A selected ion flow tube (SIFT), study of the reactions of H_3O^+, NO^+ and $O_2{}^+$ ions with a series of alkenes; in support of SIFT-MS. *Int. J. Mass. Spectrom.* **2002**, *218*, 87–101. [CrossRef]
45. Wang, T.; Španěl, P.; Smith, D. Selected ion flow tube, SIFT, studies of the reactions of H_3O^+, NO^+ and $O_2{}^+$ with eleven $C_{10}H_{16}$ monoterpenes. *Int. J. Mass Spectrom.* **2003**, *228*, 117–126. [CrossRef]
46. Smith, D.; Španěl, P.; Dryahina, K. H_3O^+, NO^+ and $O_2{}^+$ reactions with saturated and unsaturated monoketones and diones; focus on hydration of product ions. *Int. J. Mass Spectrom.* **2019**, *435*, 173–180. [CrossRef]
47. Schoon, N.; Amelynck, C.; Debie, E.; Bultinck, P.; Arijs, E. A selected ion flow tube study of the reactions of H_3O^+, NO^+ and $O_2{}^+$ with a series of C_5, C_6 and C_8 unsaturated biogenic alcohols. *Int. J. Mass Spectrom.* **2007**, *263*, 127–136. [CrossRef]
48. Finlayson-Pitts, B.J.; Pitts, J.N., Jr. *Chemistry of the Upper and Lower Atmosphere: Theory, Experiments, and Applications*, 1st ed.; Elsevier: Amsterdam, The Netherlands, 1999.
49. Rodríguez, A.; Rodríguez, D.; Soto, A.; Notario, A.; Aranda, A.; Díaz-de-Mera, Y.; Bravo, I. Relative rate measurements of reactions of unsaturated alcohols with atomic chlorine as a function of temperature. *Atmos. Environ.* **2007**, *41*, 4693–4702.
50. Rodriguez, D.; Rodriguez, A.; Soto, A.; Aranda, A.; Diaz-de-Mera, Y.; Notario, A. Kinetics of the reactions of Cl atoms with 2-buten-1-ol, 2-methyl-2-propen-1-ol, and 3-methyl-2-buten-1-ol as a function of temperature. *J. Atmos. Chem.* **2008**, *59*, 187–197. [CrossRef]
51. Giri, B.R.; Roscoe, J.M. Kinetics of the reactions of Cl atoms with several ethers. *J. Phys. Chem. A* **2014**, *114*, 8369–8375. [CrossRef]
52. Alwe, H.D.; Walawalkar, M.; Sharma, A.; Pushpa, K.K.; Dhanya, S.; Naik, P.D. Rate Coefficients for the Gas-Phase Reactions of Chlorine Atoms with Cyclic Ethers at 298 K. *Int. J. Chem. Kinet.* **2013**, *45*, 295–305. [CrossRef]
53. Andersen, C.; Nielsen, O.J.; Østerstrøm, F.F.; Ausmeel, S.; Nilsson, E.J.; Sulbaek Andersen, M.P. Atmospheric Chemistry of Tetrahydrofuran, 2-Methyltetrahydrofuran, and 2, 5-Dimethyltetrahydrofuran: Kinetics of Reactions with Chlorine Atoms, OD Radicals, and Ozone. *J. Phys. Chem. A* **2016**, *120*, 7320–7326. [CrossRef] [PubMed]

54. Atkinson, R.; Baulch, D.L.; Cox, R.A.; Crowley, J.N.; Hampson, R.F.; Hynes, R.G.; Jenkin, M.E.; Rossi, M.J.; Troe, J. IUPAC Subcommittee, Evaluated kinetic and photochemical data for atmospheric chemistry: Volume II – gas phase reactions of organic species. *Atmos. Chem. Phys.* **2006**, *6*, 3625–4055. [CrossRef]
55. Aschmann, S.M.; Atkinson, R. Rate constants for the gas-phase reactions of alkanes with Cl atoms at 296±2 K. *Int. J. Chem. Kinet.* **1995**, *27*, 613–622. [CrossRef]
56. Hooshiyar, P.A.; Niki, H. Rate constants for the gas-phase reactions of Cl-atoms with C_2 - C_8 alkanes at T= 296±2 K. *Int. J. Chem. Kinet.* **1995**, *27*, 1197–1206. [CrossRef]
57. Iannone, R.; Anderson, R.S.; Vogel, A.; Eby, P.S.; Whiticar, M.J.; Rudolph, J. The hydrogen kinetic isotope effects of the reactions of n-alkanes with chlorine atoms in the gas phase. *J. Atmos. Chem.* **2005**, *50*, 121–138. [CrossRef]
58. Li, Z.; Pirasteh, A. Kinetic study of the reactions of atomic chlorine with several volatile organic compounds at 240–340 K. *Int. J. Chem. Kinet.* **2006**, *38*, 386–398. [CrossRef]
59. Anderson, R.S.; Huang, L.; Iannone, R.; Rudolph, J. Measurements of the $^{12}C/^{13}C$ kinetic isotope effects in the gas-phase reactions of light alkanes with chlorine atoms. *J. Phys. Chem. A* **2007**, *111*, 495–504. [CrossRef]
60. Wayne, R.P.; Barnes, I.; Biggs, P.; Burrows, J.P.; Canosa-Mas, C.E.; Hjorth, J.; Le Bras, G.; Moortgat, G.K.; Perner, D.; Poulet, G.; et al. The nitrate radical: Physics, chemistry, and the atmosphere. *Atmos. Environ. Part A Gen. Top.* **1991**, *25*, 1–203. [CrossRef]
61. Barbosa, T.S.; Barrera, J.A.; Toro, R.J.; Bauerfeldt, G.F.; Arbilla, G.; Lane, S.I. Rate Coefficient for the Reaction of Cl Atoms with cis-3-Hexene at 296±2 K. *J. Braz. Chem. Soc.* **2017**, *28*, 2267–2274. [CrossRef]
62. Liang, P.; Mu, Y.J.; Daële, V.; Mellouki, A. Kinetic studies of Cl reactions with 3-buten-1-ol and 2-buten-1-ol over the temperature range 298–363 K. *Chem. Phys. Lett.* **2011**, *502*, 154–158. [CrossRef]
63. Nelson, L.; Rattigan, O.; Neavyn, R.; Sidebottom, H.; Treacy, J.; Nielsen, O.J. Absolute and relative rate constants for the reactions of hydroxyl radicals and chlorine atoms with a series of aliphatic alcohols and ethers at 298 K. *Int. J. Chem. Kinet.* **1990**, *22*, 1111–1126. [CrossRef]
64. Atkinson, R.; Aschmann, S.M. Kinetics of the gas phase reaction of Cl atoms with a series of organics at 296±2 K and atmospheric pressure. *Int. J. Chem. Kinet.* **1985**, *17*, 33–41. [CrossRef]
65. Coquet, S.; Ariya, P.A. Kinetics of the gas-phase reactions of Cl atom with selected C_2–C_5 unsaturated hydrocarbons at 283 < T < 323 K. *Int. J. Chem. Kinet.* **2000**, *32*, 478–484.
66. Walavalkar, M.; Sharma, A.; Alwe, H.D.; Pushpa, K.K.; Dhanya, S.; Naik, P.D.; Bajaj, P.N. Cl atom initiated oxidation of 1-alkenes under atmospheric conditions. *Atmos. Environ.* **2013**, *67*, 93–100. [CrossRef]
67. Kaiser, E.W.; Wallington, T.J. Pressure dependence of the reaction Cl + C_3H_6. *J. Phys. Chem.* **1996**, *100*, 9788–9793. [CrossRef]
68. Papagni, C.; Arey, J.; Atkinson, R. Rate constants for the gas-phase reactions of OH radicals with a series of unsaturated alcohols. *Int. J. Chem. Kinet.* **2001**, *33*, 142–147. [CrossRef]
69. Wingenter, O.W.; Kubo, M.K.; Blake, N.J.; Smith, T., Jr.; Blake, D.R.; Rowland, F.S. Hydrocarbon and halocarbon measurements as photochemical and dynamical indicators of atmospheric hydroxyl, atomic chlorine, and vertical mixing obtained during Lagrangian flights. *J. Geophys. Res. Atmos.* **1996**, *101*, 4331–4340. [CrossRef]
70. Riedel, T.P.; Wagner, N.L.; Dubé, W.P.; Middlebrook, A.M.; Young, C.J.; Öztürk, F.; Bahreini, R.; VandenBoer, T.C.; Wolfe, D.E.; Williams, E.J.; et al. Chlorine activation within urban or power plant plumes: Vertically resolved $ClNO_2$ and Cl_2 measurements from a tall tower in a polluted continental setting. *J. Geophys. Res. Atmos.* **2013**, *118*, 8702–8715. [CrossRef]
71. Logan, J.A. Tropospheric ozone: Seasonal behavior, trends, and anthropogenic influence. *J. Geophys. Res. Atmos.* **1985**, *90*, 10463–10482. [CrossRef]
72. Shu, Y.; Atkinson, R. Atmospheric lifetimes and fates of a series of sesquiterpenes. *J. Geophys. Res. Atmos.* **1995**, *100*, 7275–7281. [CrossRef]
73. Hein, R.; Crutzen, P.J.; Heimann, M. An inverse modeling approach to investigate the global atmospheric methane cycle. *Glob. Biogeochem. Cycles* **1997**, *11*, 43–76. [CrossRef]
74. Pfrang, C.; Martin, R.S.; Canosa-Mas, C.E.; Wayne, R.P. Gas-phase reactions of NO_3 and N_2O_5 with (Z)-hex-4-en-1-ol, (Z)-hex-3-en-1-ol ('leaf alcohol'), (E)-hex-3-en-1-ol, (Z)-hex-2-en-1-ol and (E)-hex-2-en-1-ol. *Phys. Chem. Chem. Phys.* **2006**, *8*, 354–363. [CrossRef] [PubMed]
75. Gibilisco, R.G.; Santiago, A.N.; Teruel, M.A. OH-initiated degradation of a series of hexenols in the troposphere. Rate coefficients at 298 K and 1 atm. *Atmos. Environ.* **2013**, *77*, 358–364. [CrossRef]

76. Gibilisco, R.G.; Blanco, M.B.; Bejan, I.; Barnes, I.; Wiesen, P.; Teruel, M.A. Atmospheric sink of (E)-3-hexen-1-ol, (Z)-3-hepten-1-ol, and (Z)-3-octen-1-ol: Rate coefficients and mechanisms of the OH-radical initiated degradation. *Environ. Sci. Technol.* **2015**, *49*, 7717–7725. [CrossRef] [PubMed]
77. Peirone, S.A.; Barrera, J.A.; Taccone, R.A.; Cometto, P.M.; Lane, S.I. Relative rate coefficient measurements of OH radical reactions with (Z)-2-hexen-1-ol and (E)-3-hexen-1-ol under simulated atmospheric conditions. *Atmos. Environ.* **2014**, *85*, 92–98. [CrossRef]
78. Atkinson, R.; Arey, J.; Aschmann, S.M.; Corchnoy, S.B.; Shu, Y. Rate constants for the gas-phase reactions of cis-3-hexen-1-ol, cis-3-hexenylacetate, trans-2-hexenal, and linalool with OH and NO_3 radicals and O_3 at 296±2 K, and OH radical formation yields from the O3 reactions. *Int. J. Chem. Kinet.* **1995**, *27*, 941–955. [CrossRef]
79. Jimenez, E.; Lanza, B.; Antinolo, M.; Albaladejo, J. Photooxidation of leaf-wound oxygenated compounds, 1-penten-3-ol,(Z)-3-hexen-1-ol, and 1-penten-3-one, initiated by OH radicals and sunlight. *Environ. Sci. Technol.* **2009**, *43*, 1831–1837. [CrossRef]
80. Davis, M.E.; Burkholder, J.B. Rate coefficients for the gas-phase reaction of OH with (Z)-3-hexen-1-ol, 1-penten-3-ol, (E)-2-penten-1-ol, and (E)-2-hexen-1-ol between 243 and 404 K. *Atmos. Chem. Phys.* **2011**, *11*, 3347.
81. Faxon, C.B.; Allen, D.T. Chlorine chemistry in urban atmospheres: A review. *Environ. Chem.* **2013**, *10*, 221–233. [CrossRef]
82. Breton, M.L.; Hallquist, Å.M.; Pathak, R.K.; Simpson, D.; Wang, Y.; Johansson, J.; Zheng, J.; Yang, Y.; Shang, D.; Wang, H.; et al. Chlorine oxidation of VOCs at a semi-rural site in Beijing: Significant chlorine liberation from $ClNO_2$ and subsequent gas-and particle-phase Cl–VOC production. *Atmos. Chem. Phys.* **2018**, *18*, 13013–13030. [CrossRef]

© 2020 by the authors. Licensee MDPI, Basel, Switzerland. This article is an open access article distributed under the terms and conditions of the Creative Commons Attribution (CC BY) license (http://creativecommons.org/licenses/by/4.0/).